Research
A SCIENCE PARTNER JOURNAL

REVIEW ARTICLE

Polymer Separators and Solid Polymer Electrolytes for Lithium-Metal Batteries

Kangjie Zhou[1,2], Yinjing Luo[1], Hui Zheng[3], Longsheng Zhang[1*], and Tianxi Liu[1]

[1]Key Laboratory of Synthetic and Biological Colloids, Ministry of Education, School of Chemical and Material Engineering, Jiangnan University, Wuxi 214122, China. [2]School of Materials Science and Engineering, Sun Yat-Sen University, Guangzhou 510275, China. [3]Department of Chemical and Petroleum Engineering, University of Calgary, Calgary T2N 1N4, Canada.

*Address correspondence to: zhangls@jiangnan.edu.cn

Citation: Zhou K, Luo Y, Zheng H, Zhang L, Liu T. Polymer Separators and Solid Polymer Electrolytes for Lithium-Metal Batteries. *Research* 2026;9:Article 1434. https://doi.org/10.34133/research.1434

Submitted 18 June 2026
Revised 25 August 2026
Accepted 26 August 2026
Published 22 September 2026

Copyright © 2026 Kangjie Zhou et al. Exclusive licensee Science and Technology Review Publishing House. No claim to original U.S. Government Works. Distributed under a Creative Commons Attribution License (CC BY 4.0).

Developing high-performance and high-safety lithium-metal batteries (LMBs) is of importance to meet the growing demands of next-generation energy storage. Leveraging the high structural tunability and chemical versatility of polymer materials, rational design strategies for advanced polymer separators and solid polymer electrolytes have attracted considerable attention, showing great promise for enabling LMBs with enhanced safety and reliability. This review summarizes previously reported design strategies for these key components, highlighting how molecular and microstructural engineering of polymers can address core challenges such as lithium dendrite growth and thermal instability. Recent advancements on the polymer design strategies were systematically analyzed with an emphasis on the underlying mechanisms in regulating ion transport, suppressing dendrite growth, and enhancing operation safety. Finally, current challenges and future perspectives are discussed, which aim at deepening the insight into rational design of polymer separators and solid polymer electrolyte toward further advancement and practical applications of LMBs.

Introduction

Energy storage devices are currently confronted with a dilemma arising from increasing energy demand and theoretical energy-density limitations of lithium-ion batteries and supercapacitors [1–4]. The energy densities of the lithium-ion batteries are approaching its theoretical upper limit accumulated by amounts of innovative researches, and it is still insufficient to meet the emerging requirements across the fields of energy storage and conversion [5,6]. Lithium-metal batteries (LMBs), employing high theoretical-specific-capacity lithium metal (3,860 mAh/g) as anode, demonstrate extensive potentials compared with the lithium-ion batteries [7–9]. Distinct from the intercalation/deintercalation mechanism of conventional lithium-ion batteries, LMBs realizes charge/discharge process via the repeated lithium deposition/stripping behavior on the surface of metal anode [10]. However, in the LMBs, the metal anode would generate uncontrolled dendritic lithium, owing to multiple factors such as nonuniform Li^+ distribution and the instability of the solid-electrolyte interface (SEI) layer induced by uneven Li surface [11]. For practical operation, the dendritic lithium growth may markedly influence cycling stability, while dendrite fracture further induces capacity fading and lowers Coulombic efficiency [12,13]. Moreover, the sharp lithium dendrites on anode may penetrate the separator, resulting in internal short circuits and thermal runaway of LMBs [13,14]. The existing safety concerns above are the primary obstacles for the application of LMBs.

Separators or solid-state electrolytes are indispensable components of LMBs, playing critical function of physically isolating the electrodes and regulating ion transport, which can indirectly influence the lithium dendritic growth [10]. However, the commercial polyolefin-based separator has poor compatibility with the electrolyte and dimensional instability under 200 to 250 °C [15–17]. For solid-state electrolytes, poor interface contacts with electrodes, especially at solid-state ceramic electrolytes, induce high interface resistance, thereby reducing the rate performance and lifespan of LMBs [18–20]. Currently, various strategies have emerged to resolve the existing problems above, such as developing advanced functionalized separator or further exploiting solid polymer electrolytes (SPEs) featuring excellent interfacial performance, where the polymer design strategy has been deemed as a general and effective method for developing the separator and SPEs owing to the polymer's high structural tunability and chemical versatility [21–23]. Focusing on several practical applications of energy storage requirements, amounts of function's enhancements can be facilely realized through the polymer design strategy, such as end-group graft in high-voltage poly(ethylene oxide) (PEO)-based SPEs or functionalized Li regulation group modification in the dendrite-free separator [24,25]. By exploiting the designable and functionalized polymer materials, it is feasible to improve the shortcomings of commercial separators and develop advanced SPEs [26,27].

Therefore, this review summarizes the developments of polymer design strategies employed in the advanced separator

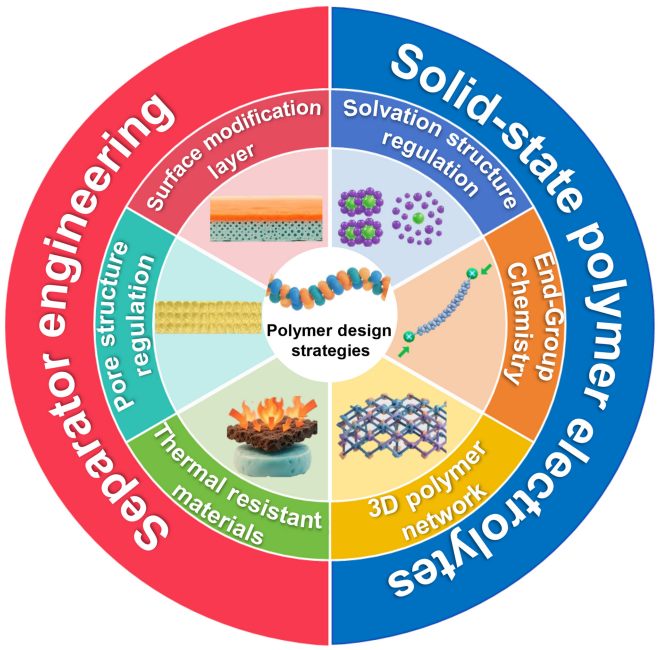


Fig. 1. Schematic overview of polymer design strategies for separator engineering and SPEs. The performance and safety of LMBs can be improved through surface modification layer, pore structure regulation, thermal resistant materials, solvation structure regulation, end-group chemistry, and 3D polymer network.

and solid-state electrolytes based on PEO materials of LMBs. We focus on how change of polymer materials including structure and groups defines the performance of both the separator and SPEs. Introducing rational design and underlying mechanism of polymer design strategies, this review discussed several advances reported recently on function-oriented separators (ion transport regulation, lithium dendrite inhibition, and thermal safety) and performance-oriented SPEs (high ionic conductivity, high voltage, and safety) involving polymer materials (Fig. 1) [28,29]. Specifically, how molecular and microstructural engineering of polymers can address core challenges such as uncontrolled lithium dendrite growth and thermal instability was comprehensively analyzed. Our goal is to connect advances in materials science with existing hazards of LMBs, providing guidelines for developing safe and high-performance LMBs. Finally, we concluded the main research pathway for the advanced separator or PEO-based SPEs through the rational polymer design strategy, providing an outlook for further development of safety and high-performance LMBs.

Design Strategy of Polymer Separator

Separator is essential elements of LMBs, which allows ion to freely transport inside pore structure of the separator [30,31]. The commercial separator is generally fabricated by polymer materials, such as polyolefin, exhibiting chemical stability and low cost for the battery separator [32,33]. However, its low melting point (≈170 °C) and high surface energy limit the integrated stability under wide temperature and compatibility with the electrolyte, which will induce the safety hazard and poor electrochemical performance [34,35]. Therefore, employing polymer design strategies to develop advanced separators is recognized as an effective method for improving the performance, safety, and efficiency of LMBs. For example, utilizing polar polymers with electrolyte affinity, the separator–electrolyte interface can be effectively improved [36]. For the safety of LMBs, heat-resistant polymers can also be used to prepare high-temperature-resistant safety separators, suitable for safe battery use under wide temperature range conditions [37,38].

Herein, various design strategies for heat-resistant polymers or polar polymers, including grafting, blending, and post-treatment, can be employed to enhance the electrochemical performance while improving the safety of LMBs. According to improvement direction, currently polymer design strategies for separator engineering can be generally divided into 2 categories: (a) enhance electrochemical performance of the separator to improve battery parameters, and (b) optimize the thermal property of the separator to broaden battery application scope. Among them, the polymer's category, structure, and porosity are precisely regulated to improve the key physical and chemical properties of the as-obtained separator [39–41]. These purposefully designed multifunctional separators unlock great potential for practical use in high-performance and safe LMBs. Building on this framework, the following section will systematically discuss recent advancements in multifunctional polymer separators, highlighting the role of polymer design strategies for improving the performance of LMBs.

Ion Transport Regulation of Polymer Separator

As an inherently electrically insulating, the separator primarily relies on the electrolyte confined within its micro- or nanometer-scale pores to conduct ions. Consequently, these ion transport behaviors occurring in the separator [ionic conductivity, Li^+ transference number (t_{Li+}), and flux uniformity] determined the overall electrochemical performance of LMBs [42–44]. Ions in the electrolyte pass through the electrolyte–separator interface and migrate repeatedly between the positive and negative electrodes. Among ion transport process, interfacial compatibility between the separator and electrolyte stands out as a crucial property that directly determines the interfacial impedance and rate capability of LMBs [45,46]. The polyolefin separators generally show poor interfacial compatibilities for carbonate-based electrolytes, resulting in high interface resistance and slow ion kinetics. Under molecular dynamics simulations, it is identified that the weak interaction between polyethylene (PE) films and ionic solutions does not cause biased distributions of ionic solutions during the diffusion process [47]. By tailoring the separator's surface properties and chemical functionality, the optimized electrolyte wettability can greatly improve the interfacial compatibility between the separator and the electrolyte, thereby minimizing the interfacial resistance of LMBs and facilitating the rapid ion kinetics.

Taking the introduction of specific polar functional groups as an example, the -SO_3Li group not only possesses a strongly polar sulfonic acid group, capable of forming a strong dipole–dipole interaction with the carbonyl group in carbonate molecules, but also serves as an immobilized anion site, inhibiting anion migration and attracting Li^+ through electrostatic repulsion effects, thereby constructing an interfacial environment conducive to the rapid transport of Li^+ at the molecular level. Specifically, the polar -SO_3Li groups serve as external anion traps, which locally deplete free anions and solvent molecules near the interface, thereby regulating the local solvation structure toward a higher proportion of contact ion pair (CIP) and aggregate (AGG). Groups represented by -COOH and -NH_2

can form a hydrogen bond network with carbonate solvent molecules and regulate the local solvation structure, greatly reducing the contact angle of the electrolyte on the separator surface and decreasing the formation of solvent-ion coordination. Based on these principles, Fan et al. [41] developed a supramolecular elastomer (ca. 3.2 μm) composed of polycaprolactone diol, tartaric acid, and 3-aminophenylboronic acid, which was coated on polypropylene (PP) separators. The separator-enriched -COOH and -NH_2 exhibit a high ionic conductivity of 0.79 mS/cm and t_{Li+} of 0.64. The calculation of desolvation energy further indicates that the -COOH group contributes to the anchoring of PF_6^-, while the desolvation energy of Li^+ for amino-containing groups is lower than that for -COOH groups (Fig. 2A). Specifically, the urea/carbamate has stronger ability of binding with Li than the solvent, which may participate in the Li^+ desolvation and compete with solvent molecules for coordination to release more Li^+. The comprehensive results confirm that the as-obtained coating exhibits excellent Li^+ regulation capacity and actively participates in Li^+ solvation sheath formation [41]. Similarly, Liang et al. [48] constructed an enriched carbonyl layer (ca. 3 μm) in a polyether sulfone-based separator as a "multi-carbonyl sites" strategy. These carbonyl sites facilitate the rapid Li^+ transport (Fig. 2B), achieving a high ionic conductivity of over 1.0 mS/cm.

Although constructing a modified layer directly on the surface of the separator through casting technology can effectively improve the interfacial performance, this strategy still has several limitations in practical applications, especially in terms of thickness control and sacrificing volumetric energy density. When forming a functional modified layer on the separator through casting methods such as scraping, dipping, or spin coating, it is inevitable to introduce an additional coating of a certain thickness. Even with careful control of the viscosity of the slurry and coating parameters, the coating thickness often reaches several micrometers or even higher, which appreciably increases the total thickness. The increase in separator thickness directly leads to a decrease in the proportion of active materials per unit volume of battery cells, resulting in a decrease in the energy density of the battery volume. Previous studies have shown that ceramic coatings with a thickness exceeding 6 μm or a thickness below 1 μm can have adverse effects on the electrochemical and thermal properties of separators [49,50]. Jung et al. [51] further discussed the influence about thickness (2 to 4 μm) of commercial Al_2O_3 coating in the separator toward thermal property and electrochemical performance of lithium battery, which could become a guide to coating technology employed in the polymer-based separator. It is suggested that 2 μm of the Al_2O_3-coating layer would be suitable for application in

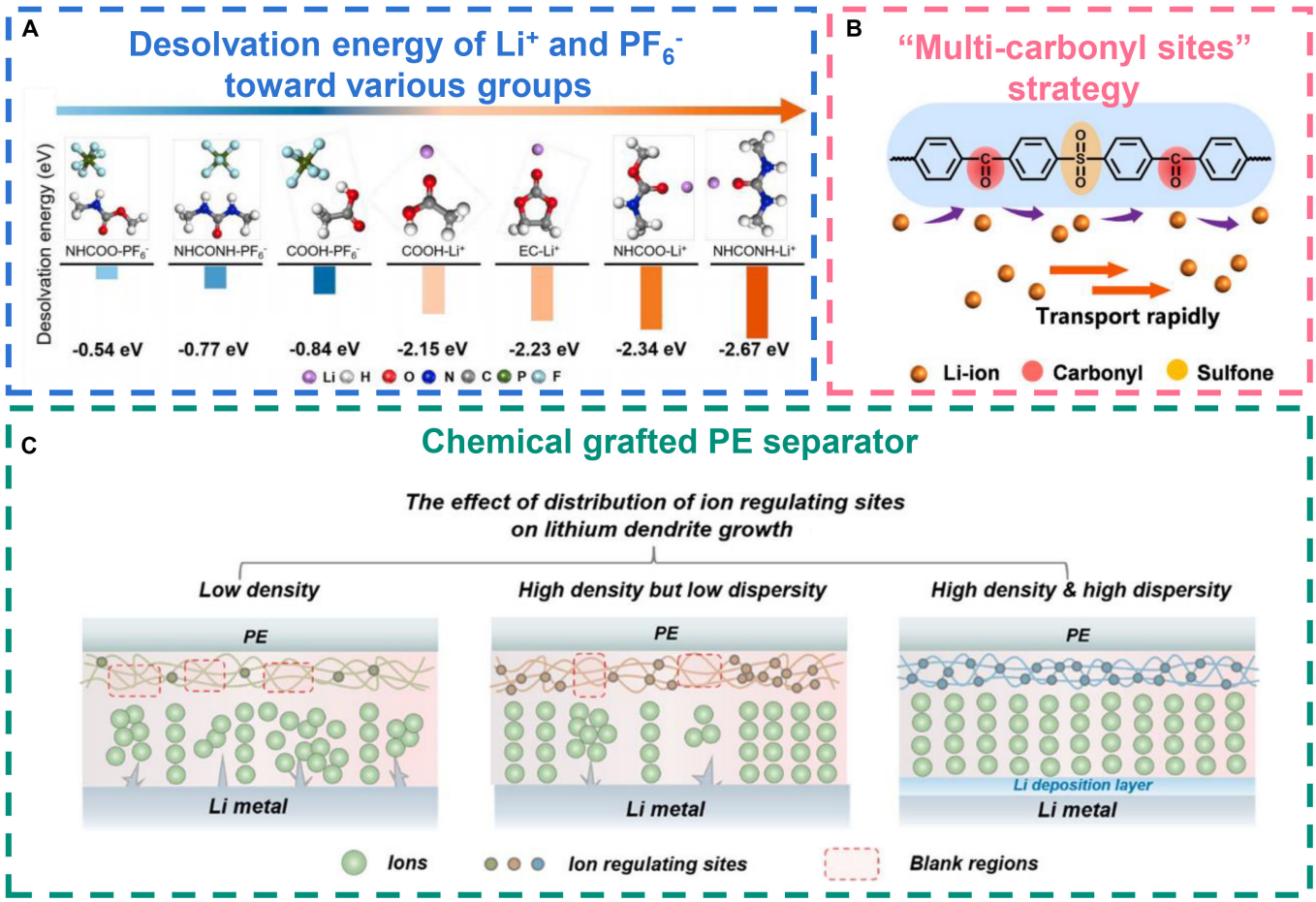


Fig. 2 (A) Calculated desolvation energy of -NHCOO, -NHCONH, -COOH, and EC toward Li^+ and PF_6^- [41]. Adapted with permission of [41]. Copyright 2025, Elsevier B.V. (B) Diagram illustrating the polyether sulfone-based separator design through a "multi-carbonyl sites" strategy [48]. Adapted with permission of [48]. Copyright 2025, Elsevier B.V. (C) Diagram of the ion transport mechanism for the hyperbranched polyamidoamine grafted PE composite separator (HBPA-g-PE) [52]. Adapted with permission of [52]. Copyright 2023, American Chemical Society.

lithium battery used for improving energy density and stability. Secondly, many coating materials that can provide excellent interface functionality are chemically incompatible with polyolefin substrates. It is usually necessary to introduce polymer binders to achieve mechanical connection between the coating and the substrate. As an inactive component, the binder may cause a decrease in the porosity of the membrane, partially masking the micropores, thereby increasing the ion transport tortuosity and interfacial resistance. In addition, long-term contact between the binder and organic electrolyte may cause swelling or dissolution, leading to unstable coating structure and performance degradation.

Different from surface coating, grafting techniques usually exhibit superior interfacial compatibility with matrix and represent a powerful tool for functionalizing separator surface, including surface-initiated polymerization, radiation grafting, plasma treatment, and chemical grafting [52]. For instance, Zheng et al. [53] fabricated an electronegative poly(pentafluorophenyl acrylate) polymer brush-grafted PP separator via surface-initiated atom transfer radical polymerization chemistry, where the PP separator was prewetted into solution containing pre-anchoring of initiators, followed by conducting a polymerization to construct one-dimensionally (1D) Li^+ flux at the nanoscale to enable rapid ion transport and ultra-stable Li deposition. While surface-initiated polymerization yields high grafting density and stable functional layers on the separator, the prerequisite pre-anchoring of initiators renders the process relatively complicated. Sun et al. [54]. prepared an F-modified poly-p-phenylene terephthamide protective layer on the PP separator via fluorine cold plasma treatment. The as-obtained separator exhibited smaller contact angle (18.5°) for the electrolyte than did the PP separator (44.1°), verifying effective surface functionalization and superior electrolyte affinity. The high-voltage $LiNi_{0.8}Co_{0.1}Mn_{0.1}O_2$ (NCM811) cell (10.77 mg/cm^2, electrolyte-to-cathode ratio = 2.3 to 3.0, 200 μm lithium metal) assembled with the as-obtained separator also exhibits superior cycling stability and practical application potential under high cathode load and lean electrolytes. From a scalable manufacturing perspective, straight forward plasma treatment and ultraviolet (UV) irradiation processes facilitate continuous production and demonstrate strong commercial potential in improving the interfacial property of the separator.

Beyond surface chemistry, the inherent pore structure characteristics of the separator, especially the pore size and porosity, play a decisive role in the ion transport dynamics, which is directly related to the migration efficiency and uniformity of Li^+ between the positive and negative electrodes. When the separator has a suitable micrometer or submicrometer pore size, the electrolyte can rapidly fill the pores under the function of capillarity and shorten the activation time, reducing the bulk resistance and achieving faster transport capable. Increasing the porosity can markedly increase the free volume occupied by the electrolyte in the separator, thus greatly improving the electrolyte absorption and retention capacity. Sufficient liquid absorption not only ensures the improvement of the ionic conductivity but also helps to form a continuous ion transport path, thus playing a key role in improving the rate performance and cycle stability. To obtain the porous polymer separator, numerous fabrication techniques are employed to construct porous structure to ensure efficient ion transport, encompassing dry-stretching, thermal-induced phase separation (TIPS), sacrificial templating, electrospinning, etc. Dry-stretching and TIPS remain the dominant processes for manufacturing the commercial polyolefin (PP and PE) separator [55]. For pore structure, the dry stretching process typically yields separators characterized by crack-like micropores and pronounced anisotropy, mainly employed to prepare the PP separator [56]. In sharp contrast, the TIPS method generates a 3D interconnected porous network while enabling the production of thinner separators compared to the dry method [57].

Notably, with the advantages of high porosity, electrospinning has emerged as a highly attractive approach of preparing the separator with 3D crosslinked pore structure due to its potential for scalable manufacturing. Driven by a high-voltage electric field, the polymer solution droplets are deformed into Taylor cones and subsequently jetted onto a collector, constantly yielding nonwoven nanofibrous membranes, with advantage of scalable production [58]. Crosslinked polymer nanofiber separators fabricated via electrospinning, such as those based on polyacrylonitrile (PAN), polyimide (PI), and polyvinyl alcohol (PVA), possess a 3D crosslinked fibrous network. Characterized by exceptional porosity and an expansive specific surface area, this unique 3D architecture secures superior electrolyte uptake and high ionic conductivity [59–74]. For example, Wang et al. [59] fabricated a composite crosslinked separator by integrating metal-organic framework (MOF) material [MIL-101(Cr)] particles into electrospun PAN nanofibers. This high-porosity framework with Cr metal sites not only realized an impressive ionic conductivity of 3.3 mS/cm but also modulated the transport of non-effective carriers through open metal sites inherent to the MIL-101(Cr) particles. Therefore, superior 3D crosslinked pore structure contributes to enlarge the effect of function-oriented design, which has potential as a framework to develop advanced polymer separators.

Beyond simply maximizing overall ionic conductivity, the ion selectivity of separators is critically related to ion transport kinetics and the rate capability of LMBs. This selectivity can be optimized by tuning the chemical composition of the separator, where Lewis acid-base interactions and electrostatic effects serve as typical principles to simultaneously enhance both ion selectivity and Li^+ conductivity [22,75]. In the functional design of membranes, Lewis acid sites refer to metal centers or electron-deficient functional groups with empty orbitals and electron pairs. Typical metal centers include Zn^{2+}, Ni^{2+}, and Al^{3+}, while electron-deficient functional groups such as boron- and aluminum-containing groups can also provide empty orbitals. These Lewis acid sites can be used as efficient anion receptors, which can be firmly anchored to the surface of the membrane channel, thus effectively limiting the free migration of anions by coordinating with the lone pair electrons of anions in the electrolyte. On the one hand, this process releases higher amount of free Li^+ ions. On the other hand, it reduces the anion migration number, substantially improving the Li^+ transference number, enhancing the dynamics of ion transportation, and improving the rate performance of LMBs. For instance, PE separators grafted with hyperbranched polyamidoamine (HBPA) possess a dense surface distribution of -NH_2 and amide (-CONH-) groups (Fig. 2C). These electron-rich sites effectively constrain anion migration while facilitating Li^+ transport through coordination effects, ultimately yielding a high t_{Li+} of 0.54 [52]. Alternatively, Wang et al. [75] developed a PE separator coated with a polyvinylidene fluoride (PVDF)/sulfonated poly(ether ether ketone) (sulfonated PEEK)-lithium blend. The intrinsic -SO_3Li groups restrict anion migration via the electrostatic

repulsion, achieving a high t_{Li+} of 0.61 while accelerating Li^+ transport through the desolvation effects. Impressively, the resulting separator enables LMBs with a high $LiFePO_4$ (LFP) loading of 10.52 mg/cm^2 to deliver stable performance for over 200 cycles, exhibiting the importance of ion transport in electrochemical performance. Electrostatic effect employs the selective repulsion or attraction of fixed charge of separator chemical groups toward ions in the electrolyte. A negatively charged transport channel can be formed by introducing a fixed negative charge group into the pore structure of the separator channel, which will electrostatically repel the anions in the electrolyte. At the same time, the charge balance allows Li^+ to pass through freely, which helps to eliminate the polarization voltage caused by the anion gradient.

The combination of chemical modification and microstructure optimization can overcome the multiple bottlenecks in Li^+ transport process. For example, in the separator matrix with high-porosity and uniform pores, anion receptors are further anchored or negative charges are fixed by chemical grafting, which ensures the rapid infiltration of the electrolyte and limits the free migration of anions, thus alleviating concentration polarization. In a word, the inherent high structural adjustability and chemical versatility of polymer materials provide a broad design space for the systematic regulation of Li^+ transport dynamics in LMBs, which has become the core starting point for improving electrochemical performance, reflecting the transformation of polymer separators from passive support components to active functional ion transport control platform.

Lithium Dendrite Inhibition of Polymer Separator

Although lithium metal possesses high theoretical specific capacity and low electrochemical potential, the uncontrollable growth of lithium dendrites severely impedes the practical application of LMBs, posing critical threats to cycling performance and safety. Fundamentally, lithium dendrite formation predominantly occurs during the charging process. Under ideal conditions, Li^+ migrating from the cathode through the separator to the anode should deposit uniformly. However, under practical conditions such as high-rate current density, low temperature, or inhomogeneous anode surface, Li^+ undergoes nonuniform reduction and deposits on localized regions of the anode surface [76]. Under high-rate conditions, the Li^+ concentration at the electrode interface drastically drops, generating a concentration gradient and a space charge layer, which substantially intensifies the local electric field. Owing to the tip effect induced by local electric field concentration, the incoming Li^+ preferentially nucleate and accelerate growth at surface protrusions, gradually evolving into sharp lithium dendrites. Ab initio molecular dynamics (AIMD) simulations reveal that, in unmodified carbonate electrolytes, CIP outnumbers solvent-separated ion pair (SSIP). CIP's heavy solvation and PF_6^- hindrance kinetically impede reductive decomposition and fluoride liberation, whereas SSIP, though rapidly decomposing, is insufficient in proportion [77]. The resulting natural SEI thus turns organic-rich, uneven, and poorly protective, fostering side reactions and dendrite growth and severely compromising battery durability. Nonuniform deposition mechanically disrupts the pristine unideal SEI layer on the anode surface, exposing fresh lithium to continuous side reactions with the electrolyte. The fractured SEI, in turn, further exacerbates nonuniform Li^+ deposition, forming a vicious cycle. Consequently, the repeated rupture and reformation of the SEI layer, together with dendrite detachment forming dead lithium, continuously consume active lithium and electrolyte, inevitably resulting in low Coulombic efficiency and rapid capacity decay.

Current polymer separator design strategies for lithium dendrite suppression are primarily focused on 2 directions: one is guiding or homogenizing Li^+ flux distribution through physical or chemical approaches of the separator, eliminating localized Li^+ concentration hotspots and inducing uniform lithium metal deposition. For example, in a high-fidelity phase-field model coupled with effective Li^+ diffusion and conductivity in multi-phase systems, it is confirmed that more uniform coating nanoparticles on the separator are effective for proactive lithium dendrite regulation [78]. The other is enhancing ion selectivity that endows the separator with preferential Li^+ conduction capability while restricting the free migration of anions through chemical modification, thereby elevating the Li^+ transference number. As depicted in Fig. 3A, theoretical calculations based on quantum chemistry showed that separators possessing large pore sizes are prone to inducing nonuniform lithium deposition, triggering the risk of Li dendrite penetration [79]. Conversely, a more concentrated and smaller pore size distribution promotes a uniform Li^+ flux, eventually facilitating a dense and homogeneous lithium anode surface. This result identified that a smaller and uniform pore distribution contribute to facilitate even lithium deposition, eventually inhibiting Li dendrite growth. Therefore, tailoring the pore architecture of polymer separators emerges as an effective approach to inhibit lithium dendrite growth on anode. Employing this pore-regulation strategy, Wang et al. [80] prepared a PI sandwiched separator featuring a PI nanofiber (PIF) middle layer for fast transport and a PI aerogel (PIA) coating with a smaller and uniform pore size of ≈150 nm. By optimizing the pore distribution of the initial PIF separator, the PIA layers enable the stable lithium anode surface at 5 mA/cm^2 and 5 mAh/cm^2 for 1,500 h, with little dendritic lithium produced in lithium cells in 200 h (Fig. 3B). Further minimizing pore dimensions, Guo et al. [81] prepared a PLA-b-PI-b-PLA triblock copolymer shown in Fig. 3C, utilizing polylactide (PLA) as a sacrificial template. Through a controlled thermal treatment process to slowly remove the PLA blocks, a mesoporous PI separator with a pore size of approximately 21 nm was obtained. The homogeneous pore size facilitates uniform Li deposition, which effectively validates the physical regulatory role of pore size in controlling lithium deposition. Although the separator with small pore size can inhibit lithium dendrite growth, the reduction of the membrane bulk pore size usually leads to a decrease in porosity, which in turn affects the bulk ion conductivity. Therefore, the pore size design of the separator is a carefully selected trade-off. Comprehensively considering both the Li-ion transmission efficiency and dendrite growth into consideration, Li et al. [81] revealed that a separator porosity within 40% to 50% is suggested for polymer separator design. Remarkably, Sheng et al. [82] found a phenomenon about pore size that a nanostructured photoresist layer (1.41 to 2.77 nm) can partially remove solvent molecules from its primary solvation sheath, suppressing the reactivity between Li^0 and carbonate electrolyte.

Beyond physical regulation to ion flux via the pore structure optimization, leveraging the chemical interactions between the

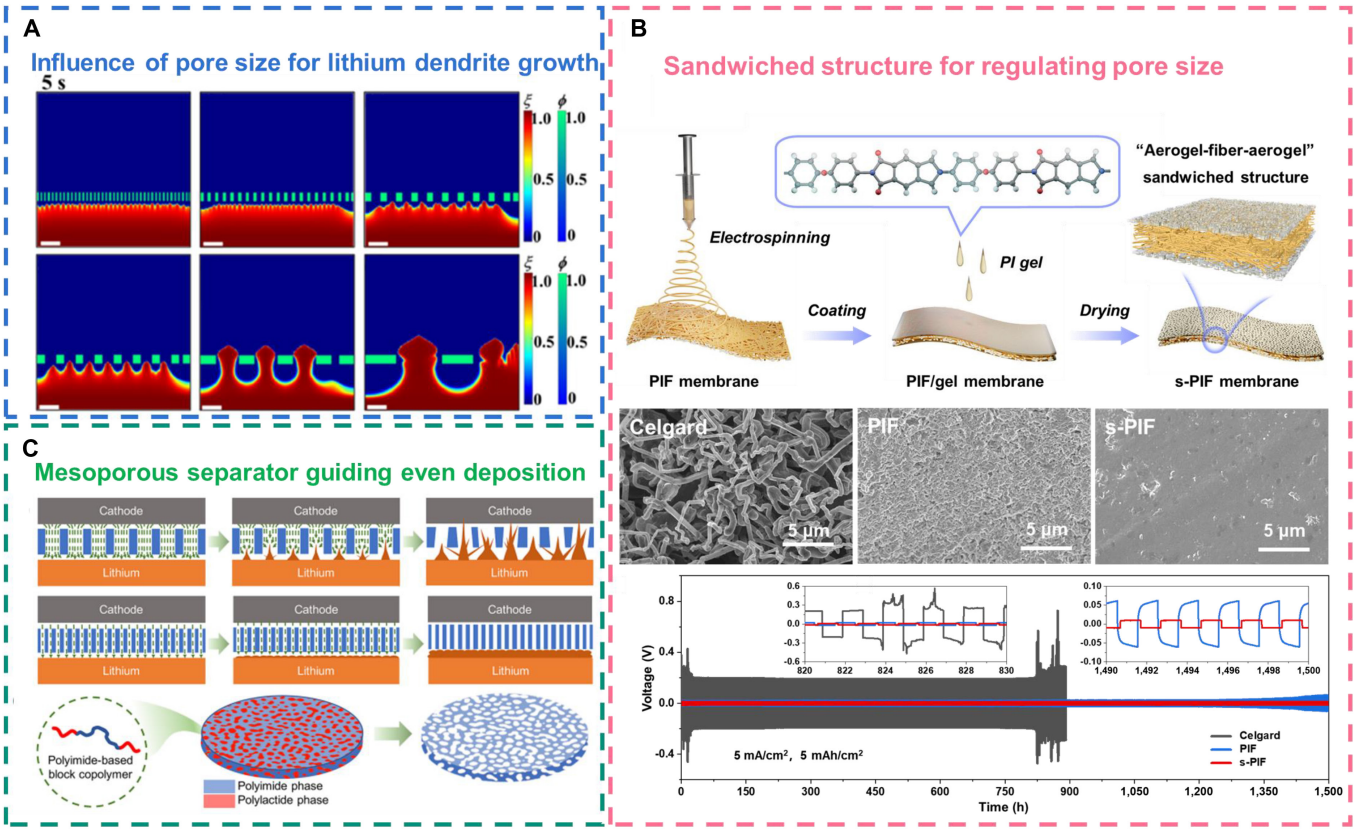


Fig. 3. (A) Theoretical calculations illustrating the relationship between pore sizes of the separator and dendritic lithium growth [79]. Adapted with permission of [79]. Copyright 2022, Elsevier B.V. (B) Fabrication process of PI aerogel (PIA)-modified separators (depicted as s-PIF). Voltage–time curves of lithium symmetrical cells with PP, PI nanofiber (PIF) separator, and s-PIF tested in 5 mA/cm^2 and 5 mAh/cm^2, and microstructure of cycled Li metal anode [80]. Adapted with permission of [80]. Copyright 2024, Elsevier B.V. (C) Effects of pore size and modulus of separators on dendrite suppression and route to prepare PI-based block copolymer [81]. Adapted with permission of [81]. Copyright 2024, American Chemical Society.

separator and Li^+ or their solvation structures in the electrolyte to actively modulate ion transport kinetics and lithium metal nucleation behavior represents another promising strategy. For instance, Ding et al. [83] developed a functional PIA separator featuring precisely tailored nitrogen sites, specifically abundant imine (C=N) and tertiary amine groups. Owing to the differences in electron cloud density distribution of various N-based chemical sites, the PIA separator can attract and repulse Li through electrostatic interactions, facilitating the interfacial Li^+ diffusion and 2D Li nucleation behavior (Fig. 4A). The high-cathode-loading LFP cells (12.0 mg/cm^2) with the PIA separator can realize stability cycling over 200 cycles, superior than that with the PP separator. Harnessing similar nitrogen chemistries, Che et al. [84] employed interfacial polymerization to grow a polypyrrole (PPy) layer on one side of a nanoporous PVDF membrane (Fig. 4B), generating a Janus separator. Enriched with nitrogen-containing functional groups (specifically pyrrolic-N), the PPy layer provides active nucleation sites for Li^+ deposition on the separator surface, effectively guiding the lateral growth of lithium dendrites.

Except directly introducing the chemical group to regulate Li^+ flux, altering ion selectivity of the separator is another pathway to influence lithium dendrite nucleation through chemical interactions or the polymer structure design. The t_{Li+} of the separator is an ion selectivity parameter closely related to the growth of lithium dendrites, which is the fraction of the current carried by Li^+ in the total current. It is commonly measured by the Bruce–Vincent potentiostatic polarization method, followed by calculating through the following formula:

$$t_{Li^+} = \frac{I_{ss}\left(\Delta V - I_0 R_0\right)}{I_0\left(\Delta V - I_{ss} R_{ss}\right)} \quad (1)$$

where I_0 and I_{ss} are the initial current and steady state current, respectively. The interface impedance between the electrolyte and electrode was measured before R_0 and after polarization R_{ss}. ΔV is the applied constant potential.

According to the classical sand time model and chazalviel space charge theory, increasing t_{Li+} can effectively prolong the initial time of dendrite nucleation τ by reducing the number of anion migration, reducing the thickness of the space charge layer at the electrode interface and the local electric field strength. According to the Sand's time model, the onset time τ of lithium dendrite nucleation under galvanostatic conditions is given by:

$$\tau = \frac{\pi D\left(eC_0\right)^2}{4J^2\left(1 - t_{Li^+}\right)^2} \quad (2)$$

where D is the ion diffusion coefficient, C_0 is the initial salt concentration, e is the elementary charge, J is the effective current density, and t_{Li+} is the Li^+ transference number. The equation indicates that the nucleation time is inversely proportional

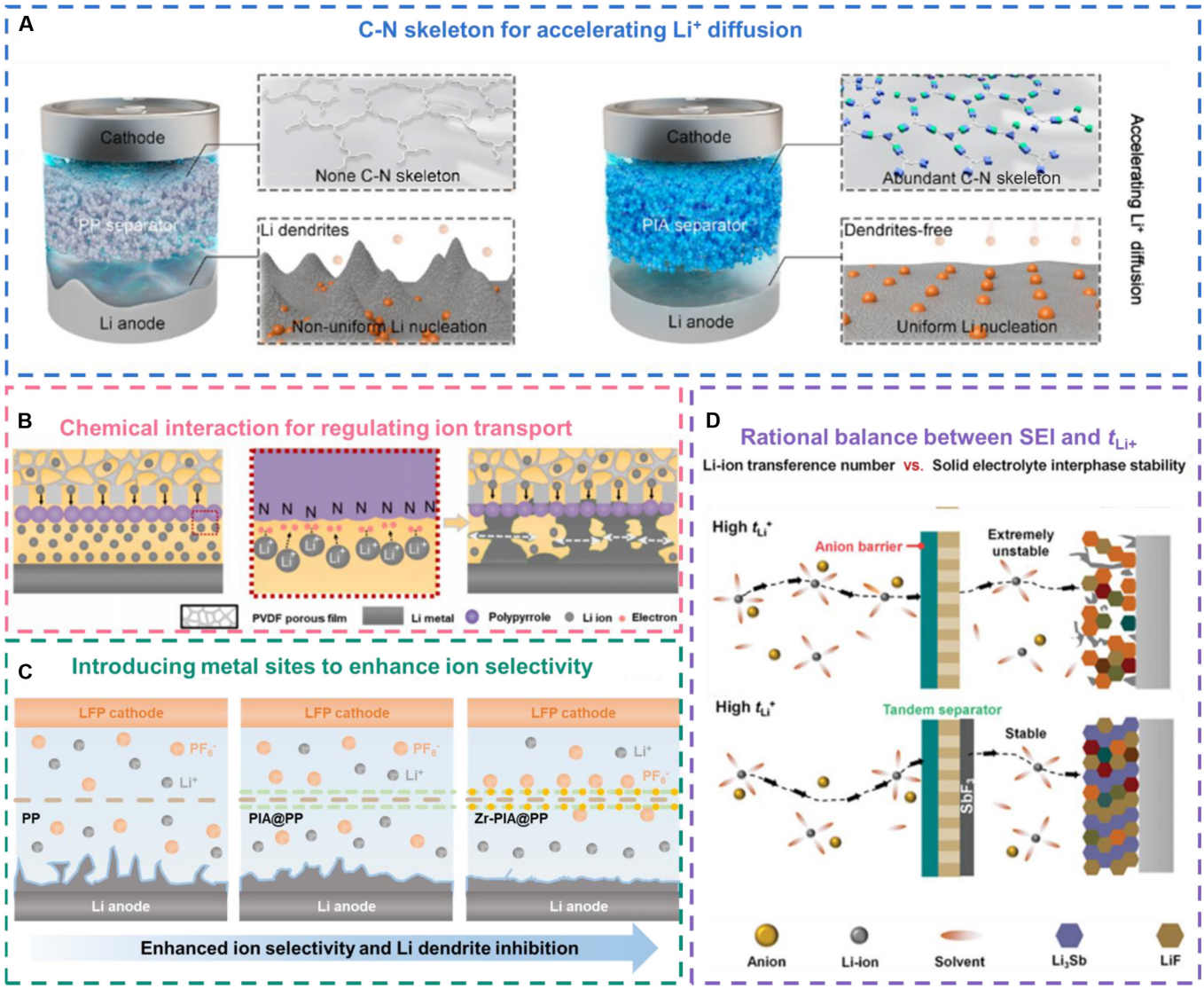


Fig. 4. (A) Schematic illustrating that the PIA separator with abundant C–N skeleton can effectively facilitate the uniform Li nucleation [83]. Adapted with permission of [83]. Copyright 2023, National Academy of Sciences. (B) Mechanism of the Janus PVDF/PPy separator for suppressing dendritic lithium [84]. Adapted with permission of [84]. Copyright 2025, Elsevier B.V. (C) Schematic of the Zr-PIA@PP separator facilitating a uniform and selective Li^+ flux on anode [85]. Adapted with permission of [85]. Copyright 2025, Wiley-VCH GmbH. (D) Schematic illustrating the mechanism of the anion-anchoring separator design and the tandem separator design [90]. Adapted with permission of [90]. Copyright 2023, Wiley-VCH GmbH.

to $(1 - t_{Li+})^2$. As t_{Li+} approaches unity, τ theoretically tends to infinity, and dendrite nucleation is substantially postponed.

Consequently, several modifications about the polymer design strategy to increase t_{Li+} of separators were developed to suppress lithium dendrite, including the incorporation of metal sites and covalent organic frameworks (COFs) [85–87]. Metal centers typically exhibit strong Lewis acidity and can coordinatively anchor anions in the electrolyte, promoting lithium salt dissociation and releasing additional free Li^+, thereby attenuating the electrostatic coupling resistance of anions to Li^+ transport and alleviating the binding interactions between Li^+ and anion in CIP. Figure 4C illustrates a functionalized separator (Zr-PIA@PP) where single-atom zirconium sites are coordinated on nanoporous PIA coating onto the PP separator. By anchoring Zr sites within the porous aerogel framework to inhibit the free transport of anion in electrolyte, the composite separator achieves a superior t_{Li+} (0.52) compared to the commercial PP separator (0.31), effectively delaying dendritic lithium nucleation [85]. Beyond the design of metal sites, the COFs with highly ordered and size-tunable sub-nanometer pores enable precise sieving to allow desolvated or partially solvated Li^+ to pass, robustly suppressing lithium dendrite growth. Jalees et al. [88] prepared a bifunctional membrane, comprising PI-COFs and polybenzimidazole (PBI), where PBI is used as membrane matrix, while the microstructure and polar functional groups of COFs regulate the flow of Li^+. The PBI separator-containing COFs exhibit high t_{Li+} (0.53) and strong ionic conductivity at room temperature under ideal electronegativity conditions, and achieve relatively uniform lithium deposition.

While high ion selectivity is desired, an excessively high t_{Li+} can be counterproductive. Specifically, the over-restriction of

anions by the separator results in an "anion-depleted" state at the anode interface, impeding the construction of a robust, inorganic-rich SEI derived from the reductive decomposition of anions. These inorganic constituents are essential for maintaining the mechanical integrity and interfacial passivation capability of the SEI. Excessively suppressing anion migration through the separator design will reduce the free anion concentration and generate the anion-depleted state in the electrolyte–anode interface, rendering organics-dominated SEI produced by solvent molecules for solvent-rich anion-depleted interface fragile and heterogeneous. Therefore, the trade-off between SEI and ion selectivity needs to be carefully considered. Zhou et al. [89] reviewed the several improvement strategies for t_{Li+} in liquid electrolytes, where statistical results of most research results showed that a t_{Li+} of ≈0.7 is beneficial for delaying the nucleation time of lithium dendrites and does not fall into an anion depleted state. Otherwise, the multiple factor design strategy for both SEI and t_{Li+} is also a promising pathway to ensure the long-term cycling for LMBs. To reconcile the competing demands of SEI robustness and high t_{Li+}, Ding et al. [90] designed an asymmetric separator (Fig. 4D), in which the cathode-facing layer restricts anions to boost Li^+ transport, while the anode-facing layer reacts with Li to generate beneficial inorganic components like Li_3Sb and LiF, reconciling the conflict between ion selectivity and SEI quality. The high-cathode-loading NCM811 cells (10 mg/cm^2) with the asymmetric separator can stabilize cycling over 150 cycles, exhibiting the practical application potential.

Based on the above analysis, the core mechanism of the polymer design to suppress lithium dendrite growth lies in the synergistic optimization of ion transport kinetics and interface stability through molecular engineering and microstructure regulation, thereby breaking the vicious cycle of uneven lithium deposition. Onone hand, by introducing fixed negative charge groups such as sulfonic acid and carboxylic acid groups on polymer chains or pore structure, or anchoring anions in electrolytes using Lewis acid sites such as metal organic frameworks, COFs, and single atom metal sites, t_{Li+} can be substantially increased. On the other hand, by constructing uniform and high-porosity nanopores, or optimizing the surface chemistry of the separator with polar functional groups and lithium affinity sites, the Li^+ flux can be made consistent within the membrane plane, eliminating the preferential nucleation hotspots induced by local Li^+ enrichment. Therefore, physical and chemical methods through polymer design strategies were effective for guiding the uniform deposition of lithium metal.

Operation Safety of Polymer Separator

Thermal stability constitutes one of the core parameters ensuring the safe operation of high-energy-density batteries. Traditional polyolefin separators, owing to their limited melting points (approximately 130 to 135 °C for PE and 165 °C for PP), are prone to severe thermal shrinkage and structural collapse under extreme thermal abuse conditions, causing direct physical contact between the cathode and anode and triggering violent internal short circuits. To effectively mitigate these safety risks, advanced design strategies for high-safety polymer separators have attracted extensive attention, among which 3 representative approaches can be identified: flame-retardant separators, separators based on thermally stable polymer matrices, and separators integrated with phase-change materials (PCMs).

Among these strategies, incorporating flame-retardant components into separator matrix offers a robust approach to arrest thermal runaway and mitigate associated catastrophic losses. Fundamentally, the flame-retardant separators suppress electrolyte combustion and the propagation of thermal runaway through the condensed-phase carbonization: Upon ignition of the separator, the flame-retardant additives will decompose at elevated temperatures to generate acidic species, which act as catalysts to facilitate the crosslinking of polymer chains, ultimately converting into a dense carbon-rich layer. The newly formed layer isolates oxygen and internal combustible components, achieving effective flame retardancy and reliable safeguards for LMBs. Representative of this flame-retardant mechanism, phosphorus-based additives like triphenyl phosphate (TPP) and ammonium polyphosphate (APP) decompose upon heating to form a dense phosphate ester layer on the material surface. This layer effectively isolates oxygen and reduces the heat release rate (HRR) of the material. Demonstrating this strategy, Chen et al. [91] reported a separator modified with the phosphorus flame-retardant polyphosphate ester shown in Fig. 5A. The introduction of flame retardant enhances the thermal safety of the as-obtained separator, which achieved a lower self-extinguishing time of 55.73 s/g and better flame-retardant property compared to pure PE separators. Similarly, Liao et al. [63] developed a multifunctional composite separator by anchoring silica microencapsulated APP particles within a PVA fiber matrix. When the battery is burning, this microencapsulated separator can achieve precise release of flame retardant, successfully delayed the ignition time of pouch cells by 138 s (Fig. 5B) and decreased the peak HRR by 23.85% (Fig. 5C). Accurate thermal shutdown is based on the precise release of thermo-sensitive materials during specific temperature. When the temperature exceeds the critical value, the pore size is blocked by thermo-sensitive materials and the ion transport channel is forcibly closed to cut off the exothermic reaction, preventing thermal runaway and improving the safety of LMBs [92,93]. Zheng et al. [94] used coaxial electrospinning technology to encapsulate the flame-retardant TPP in a PVDF shell. As obtained, 1TPP@2PVDF can achieve hot shutdown function at 177 °C and self-extinguishing time of 1.82 s, demonstrating better intelligent protection function. Yu et al. [95] coated poly(melamine terephthalamide) onto the PE separator, which participates in the decomposition of the PE separator and alleviate the degradation rate of PE chain, thereby realizing a wide-temperature-range thermal shutdown. Beyond directly introducing phosphorus-based flame retardants to the polymer, the utilization of the polymer with specific functional groups (e.g., -NH and -CF) offers another effective pathway. Representative polymer materials encompass PI, poly (vinylidene fluoride-co-hexafluoropropylene) (PVDF-HFP), polytetrafluoroethylene (PTFE), and fluorinated acrylate polymers [61,91,96,97]. Specifically, fluorinated polymer materials exhibit excellent affinity for liquid electrolytes, which can enhance the flame-retardant properties of the polymer while also demonstrating excellent interface performance, ultimately enabling the simultaneous strengthening of electrochemical performance and operation safety for LMBs. For instance, Muche et al. [61] reported a 3D cross-linked fluorinated PI/PVDF-HFP nanofiber separator, which exhibited a superior fire-extinguishing capability compared to the PP separator. Furthermore, the polar functionalities, including exposed amide (-NH) and fluoro (-CF) groups, endow the separator with an

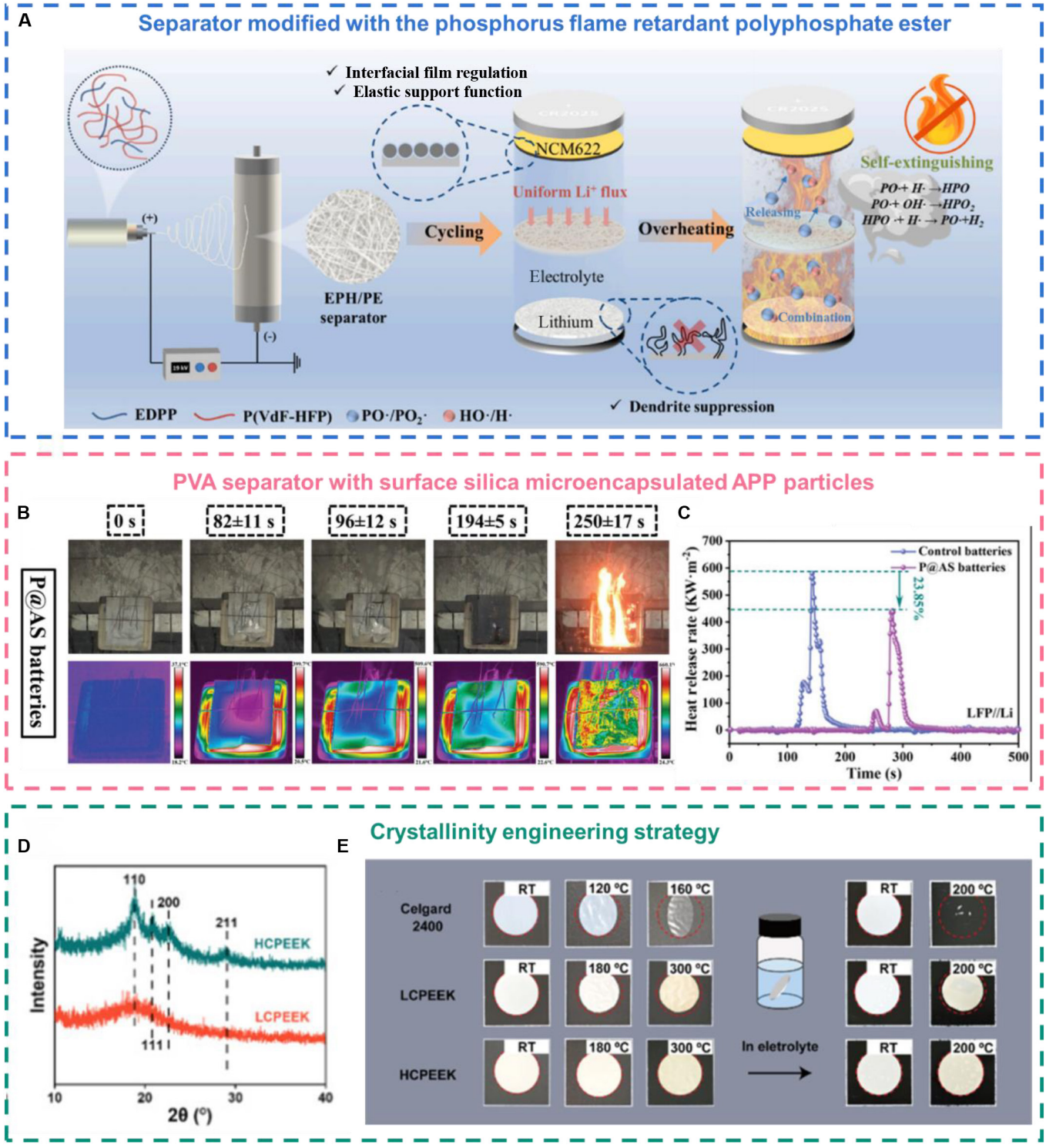


Fig. 5. (A) Preparation of the flame-retardant separator via electrospinning [91]. Adapted with permission of [91]. Copyright 2025, Elsevier B.V. (B) Digital photos and (C) HRR curves of pouch cells assembled with the separator, where surface silica (SiO_2) microencapsulated APP particles anchored in a PVA fiber matrix (P@AS-x) separator under continuous external heating [63]. Adapted with permission of [63]. Copyright 2024, Wiley-VCH GmbH. (D) XRD spectra and (E) thermal stability tests of separators with various crystallinities [98]. Adapted with permission of [98]. Copyright 2025, Elsevier B.V.

enhanced electrolyte affinity (a contact angle of 0°) and high ion selectivity, achieving a substantial t_{Li+} of 0.7.

Complementary to chemical flame retardancy, enhancing the mechanical strength and intrinsic thermal stability of the separator can effectively suppress the thermal shrinkage and melt rupture of LMBs under high-temperature conditions, where thermal stability directly determines the upper-temperature limit for maintaining dimensional integrity, and mechanical strength safeguards the separator's resistance to puncture and its ability to preserve internal pore structure, consequently

blocking cathode–anode short circuits caused by the separator structural collapse at the source and broadening the safe operating temperature window of the battery. Relevant polymer design strategies typically involve incorporating thermal stability fillers, regulating polymer crystallinity, and constructing hierarchical structures [98–100]. Regarding filler incorporation, most inorganic materials can typically withstand temperatures far exceeding those of polymer matrices while maintaining structural stability, making them ideal candidates for reinforcing polymer matrices. However, the issues of interfacial compatibility and dispersion uniformity between inorganic fillers and polymer matrices, where the former pertains to the physicochemical affinity and bonding strength between filler surfaces and polymer chainswhile the latter concerns the spatial homogeneity of filler distribution within the matrix, constitute a core challenge that must be addressed to realize high-performance composite materials. Zhang et al. [99] developed a composite separator using poly(aryl ether benzimidazole) (OPBI) and functionalized inorganic fillers of boron nitride (BN). Firstly, they carried out precise amino (-NH_2) functionalization treatment on 2D BN to prepare functionalized BN (f-BN), which solved the compatibility between the inorganic matrix and the polymer. Then, the nonsolvent induced phase separation process was employed to further optimize dispersion of f-BN particles and regulate morphology. Driven by superior thermal stability and low linear thermal expansion coefficient of both components, the resulting separator successfully maintains structural integrity even at 200 °C.

It is highly desired to regulate the intrinsic crystallinity of polymers, which presents another robust approach to bolster thermal resistance without second component. For instance, by using a precise crystallinity engineering strategy, Wang et al. [98] fabricated a semi-crystalline PEEK separator with high crystallinity (denoted as HCPEEK) . As demonstrated by x-ray diffraction patterns, the crystallinity of HCPEEK was systematically regulated via chemical modification and clamping–annealing processes (Fig. 5D). Benefiting from retaining higher crystallinity (22%) compared to its unmodified counterpart, the HCPEEK separator exhibits remarkable thermal stability up to 300 °C (Fig. 5E), which identified the possibility of developing thermal stability materials using a polymer crystallinity engineering strategy. The industry-level LFP/graphite pouch cells (graphite mass loading of 8.4 mg/cm^2, LFP mass loading of 15.5 mg/cm^2) can obtain high-capacity retention of 94% at 0.2 C, thus confirming the practical potential of the HCPEEK separator. Furthermore, focusing on the structure design, special structural design strategies exemplified by sandwich and gradient architectures can markedly enhance the comprehensive mechanical properties of separators, particularly in terms of tensile strength, puncture strength, and dimensional stability at elevated temperatures [100,101]. For example, Zhou et al. [100] reported a PI-based sandwiched composite separator incorporating cross-linked APP. This structural design maintains thermal stability at 200 °C through homogeneous PI-based sandwiched structure but also delivers enhanced flame retardance, thereby achieving the lowest total heat release among the tested samples.

As an essential complement to thermal safety strategies such as flame retardancy and thermally stable matrices, integrating PCMs into the separator matrix provides a passive latent-heat-storage-based active thermal buffering defense mechanism through intrinsic solid–liquid phase-change behavior, which can melt and absorb substantial latent heat when the temperature exceeds the phase transition point. Taking paraffin wax as an example, its melting point is approximately 45 °C and its latent heat can reach ≈240 J/g. During heating, this endothermic phase transition efficiently absorbs the heat released by thermal sources, effectively suppressing temperature spikes and delaying or even interrupting the thermal runaway chain reaction. However, the liquid leakage issue of PCMs after melting must be addressed through strategies such as hollow nanofiber encapsulation or microencapsulation. Therefore, these PCMs are typically encapsulated within thermally stable and highly conductive frameworks to minimize adverse interactions between PCMs and electrolyte [102]. For instance, Li et al. [103] prepared a PAN-based separator consisting of a heat-storing electrospun paraffin fibers and a thermally conductive hexagonal BN nanosheet modification layer. The synergistic combination of heat storage and thermal conduction endows the separator with rapid thermal responsiveness and outstanding heat mitigation capability for the in situ thermal management of LMBs (Table 1).

To sum up, the rational design of function-oriented polymer separators is paramount for simultaneously enhancing electrochemical performance and safety of LMBs. By precisely tailoring their chemical composition and micromorphology, polymer-based separators can achieve functional optimization of ionic conductivity, dendrite inhibition, and thermal stability, exhibiting the distinct potential of the polymer design for the development of high-performance, intrinsically safe separators. Fundamentally serving to regulate ion transport and isolating electrodes, polymer separators have undergone a paradigm shift, evolving from passive physical barriers into elaborately designed and safety enhanced materials. Capitalizing on the high structural tunability and chemical versatility of the polymer, advanced structural engineering and functional modifications offer a promising route for further development of high-performance, intrinsically safe separators.

Design Strategy of Solid Polymer Electrolyte

Similar to separator engineering, exploring solid-state electrolyte is also considered as another pathway to achieve advanced LMBs. Driven by the escalating demand for higher energy-density devices, solid-state electrolyte has emerged as a transformative pathway for next-generation LMBs. The solid-state electrolyte exhibits the likelihood of higher energy density than conditional liquid-electrolyte-based battery and better compatibility with high-energy-density cathode materials, which shows extensive potential in high-energy-density LMBs [104–106].

Beyond the above separator engineering and solid-state electrolytes, gel polymer electrolytes (GPEs) consist of a polymer host swollen with a liquid salt/solvent phase. For GPEs, the liquid-imbibed polymer network usually possesses sufficient polar groups to realize superior electrolyte retention, where solvent and Li salts are filled with the porous framework [107–109]. GPEs are deemed as a pragmatic intermediate offering high room-temperature ionic conductivity and higher energy density, which is closer to commercial applications than SPEs. However, it must be clarified that GPEs retain substantial volatile liquid components. Mechanistically, GPEs are essentially a hybrid architecture that combines liquid-phase ionic conduction with a solid polymeric framework, conceptually overlapping with the separator engineering in liquid systems

Table 1. Summary of the performance comparison between polymer separators

References	Sample	Polymer	t_{Li+}	Ionic conductivity (mS/cm)	Thermal shrinkage
[41]	PP-CPU	Polyurethane	0.64	0.79	Stability at 160 °C
[48]	PES2K-C	Poly(ether sulfone)	0.79	1.35	Stability at 200 °C
[177]	IISS	PE	N/A	0.464	Stability at 200 °C
[53]	PPFPA-g-Celgard	Poly(pentafluorophenyl acrylate), PP	0.61	0.833	N/A
[54]	F-PPTA@PP	Fluorinated poly(p-phenylene terephthalamide), PP	0.74	1.09	Stability at 165 °C
[59]	PANM	PAN	0.54	3.15	N/A
[52]	HBPA-g-PE	HBPA, PE	0.54	1.13	N/A
[75]	V-40-P/S@PE	PVDF, PEEK, PE	0.61	0.59	N/A
[80]	s-PIF	PI	N/A	1.2	Stability at 250 °C
[81]	Mesoporous PI	PI	N/A	N/A	N/A
[82]	Zr-MOCN@PP	Polymerized Zr-MOC photoresist (Zr-MOCN), PP	0.69	N/A	N/A
[83]	PIA separator	PI	0.78	0.92	Stability at 210 °C
[84]	Janus PVDF/PPy-0.2	PVDF, PPy	N/A	0.732	N/A
[85]	Zr-PIA@PP	Zirconium-coordinated PI, PP	0.52	0.9	Stability at 200 °C
[88]	PBI@PI-COF10	PBI, PI	0.53	1.84	Stability at 200 °C
[90]	Z5P/PE/SBF	Poly dimethyl diallyl ammonium chloride, PE	0.79	0.6	Thickness reduced from 21 to 10 μm at 160 °C
[91]	E2PH/PE	Polyphosphate ester, PVDF-HFP, PE	0.57	0.354	N/A
[63]	P@AS-10	PVA	N/A	1.475	Stability at 150 °C
[94]	1TPP@3PVDF	PVDF	N/A	0.4374	N/A
[95]	PTMs@PE	Poly(terephthaloyl-melamine), PE	0.65	1.21	<5% at 150 °C
[61]	PI/PV	Fluorinated PI, PVDF-HFP	0.7	3.3	Stability at 300 °C
[99]	OPBI@f-BN	OPBI	N/A	1.29	Stability at 200 °C
[98]	HCPEEK	Semi-crystalline PEEK	0.71	0.61	<2% at 300 °C (dry); no shrinkage at 200 °C (wetted)
[100]	PIFAP-2	PI	N/A	1	Stability at 200 °C
[103]	HCHS	PAN	0.49	0.84	Stability at 200 °C

on one hand and the polymer matrix design in solvent-free SPEs on the other. This work is dedicated to a complementary illustration of polymer engineering in liquid-based systems and SPEs. Therefore, the following sections will introduce the application of the polymer design in solid electrolytes.

Generally, according to materials categories, solid-state electrolytes are classified into solid-state ceramic electrolytes and SPEs. Solid-state ceramic electrolytes achieve conductivity through the rapid migration of specific ions within the crystal lattice, which primarily relies on the directed migration of ions within defects, vacancies, or ordered channels in the crystal structure to complete charge transport [110,111]. Currently, the solid-state electrolyte with the highest room temperature ionic conductivity is sulfide-based electrolyte, which belongs to the ceramic category [112–114]. However, solid-state ceramic materials have severe interfacial problems toward electrodes, thereby inducing high interfacial resistance and poor ion transport, which will greatly hamper the practical application of LMBs [115]. Characterized by superior flexibility and interfacial compatibility with lithium metal anode, SPEs possess the extensive potential for application in high-energy-density LMBs. Serving as the archetype for SPEs, PEO-based polymer electrolytes are the earliest developed materials and have become a prominent research focus.

The ion transport within PEO relies on the coordination between ether oxygen groups in the PEO segments and Li^+, facilitated by the segmental motion of amorphous regions. Prepared via solution casting or thermal pressing, PEO-based electrolyte membranes can realize good flexibility. However, its practical application in LMBs is heavily impeded by 3 critical

bottlenecks: (a) The sluggish ionic conductivity at room temperature (10^{-7} to 10^{-8} S/cm), arising from high crystallinity of PEO, falls far short of practical requirements of LMBs. (b) The intrinsically narrow electrochemical oxidation window (≈3.7 to 3.9 V versus Li^+/Li) of PEO impedes its compatibility with high-voltage cathode materials. (c) The insufficient mechanical strength of PEO at operating temperatures, which falls far below the mechanical threshold, makes it difficult to construct a physical barrier to effectively inhibit lithium dendrite growth. Validating the efficacy of direct chain modification, advanced polymer design strategies demonstrate immense potential in engineering high-performance and intrinsically safe PEO-based SPEs for LMBs. Addressing the challenges, this section systematically reviews recent modification strategies for PEO-based electrolytes, focusing on advancements utilizing the polymer design strategy to achieve broadened electrochemical window, enhanced ionic conductivity, and operational safety.

Ion Transport Regulation of Solid Polymer Electrolyte

Different from the ion transport occurring in electrolyte inside the separator, PEO-based SPE itself is a medium for ion conduction, where Li^+ undergoes a process of "chelation–decomplexion–migration" to achieve leapfrog migration in the PEO matrix with the assistance of the movement of segments. Solvation structure modulation serves as a similar pathway for enhancing ion conductivity in both separators and PEO-based electrolytes. For separators, ionic conductivity hinges on porosity, whereas the ion transport capability of PEO-based SPEs is strongly dependent on the crystallinity of the host matrix. Since ionic conduction is restricted primarily to the amorphous phase, minimizing PEO crystallinity is a pivotal approach to boosting ionic conductivity. Amorphous-rich PEO provides expanded pathways for Li^+ transport, delivering superior room-temperature ionic conductivity and thus accelerating the rate performance of PEO-based LMBs. Typically, differential scanning calorimetry (DSC) is utilized to assess the crystallinity of PEO-based SPEs, where a diminished melting enthalpy (ΔH_m) during the second heating cycle signifies a reduction in crystalline zones, confirming the success of crystallinity-regulation modifications. The crystallinity structural disruption can be evidenced by a downward shift in the glass transition temperature (T_g). Moreover, XRD characterization can be coupled to probe the crystalline behavior of PEO, opening avenues for maximizing ionic conductivity.

The introduction of tailored functional groups is widely adopted to further modulate ion transport or interfacial properties, such as intrinsically amorphous polymers or moieties exhibiting lower electron donor numbers than native ether oxygens. Upon the introduction of amorphous polymers, the second component's polymer chains interpenetrate the PEO chains, disrupting the regular folding of PEO segment into crystal lattices and forcibly maintaining PEO in an amorphous state. Furthermore, the inherently larger free volume of the amorphous secondary component affords expanded spatial freedom for PEO segmental mobility, thereby synergistically accelerating ion transport kinetics. As illustrated In Fig. 6A, the poly(p-phenylene benzobisoxazole) (PBO) nanofiber was introduced into the composite electrolyte as second element to diminish the crystallinity of PEO and to broaden the amorphous domains. The T_g of PEO decreased from −36 to −40 °C, effectively identifying the reduced crystallinity and resulting in a high ionic conductivity of 6.1×10^{-4} S/cm at 60 °C [116].

Fortuin et al. [117] selected PEO and poly(ε-caprolactone) (PCL; with low donor number ester groups) as comparative polymer matrices, introducing typical low donor number groups such as ester groups into the SPE system, and comprehensively verifying the regulatory effect of low donor number groups on the solvation and dissociation behavior of Li^+ from 3 aspects: coordination environment, charge carrier morphology, and ion transport kinetics. Upon introducing polymers functionalized with low-donor-number moieties (e.g., esters, carbonates, cyano groups, or fluorine atoms), the solvation structure of electrolytes can be altered, weakening the overall environmental binding force on Li^+ and lowering the dissociation energy barrier [40,118]. Furthermore, blending PEO with polymers featuring highly polar functionalities, such as polypropylene carbonate (PPC) and polyethylene glycol (PEG) derivatives, serves as a robust strategy to boost room-temperature ionic conductivity [119–121]. PPC serves as both a crystallization inhibitor and a plasticizer, aiming to reduce the crystallinity of PEO and thereby enhancing ionic conductivity [122,123]. PEG not only acts as a plasticizer, increasing the free volume of the polymer matrix and providing more migration space for Li^+ [124,125]. Based on it, Yuan et al. [126] introduced a coordination polymer Co(tpy)-PEG consisting of Co^{2+} terpyridine and PEG (Fig. 6B) into the PEO matrix, where its low crystalline PEG part can efficiently conduct Li. Notably, Co^{2+} competes with Li to interact with anions via Lewis acid-base interactions and enhance dissociation of LiTFSI and weaker interaction between Li and O atoms, leading to the release of more free Li and yielding a high ionic conductivity of 0.22 mS/cm.

Furthermore, employing polymers capable of anchoring anions in the electrolyte is another effective strategy to achieve efficient ion transport [127–129]. In the low-dielectric-constant PEO matrix, lithium salts tend to form uncharged, nonconductive CIPs or even larger ion AGGs [130,131]. When groups with strong Lewis acidity (e.g., boron-containing groups or electron-deficient aromatic rings) are introduced onto the polymer backbone, the backbone acts as anion acceptor [132–134]. According to Le Chatelier's principle, the strong interaction between the anchoring sites and anions competitively disrupts the electrostatic equilibrium between anions and cations in the electrolyte. This process substantially increases the concentration of free Li^+ in LMBs, effectively immobilizing anions to promote a higher degree of lithium salt dissociation. A variety of functional materials with capability of anchoring anions in the electrolyte were reported, including poly(2,2,6,6-tetramethyl-1-piperidinyloxy-4-yl acrylate) (PTPA) [135], PVDF-HFP/CeO_2 nanonetworks [136], covalent organic polymers (COPs) anchored with cationic chains [137], PBI [138], and allyl acetoacetate with *N*,*N*-methylenebisacrylamide [139]. For PTPA, Chen et al. [135] revealed that the radical polymer PTPA (Fig. 6C) generates strongly positive oxoammonium cations ($PTPA^+$) in situ, enhancing the release of active Li^+ through charge-dependent interactions with anions, and providing accelerated Li^+ transport pathways. For COP anchored with cationic chains, Fang et al. [137] found that the cationic groups on the branches of COPs have the ability to attract more $TFSI^-$ and release Li. The free Li passes quickly through the pores of the COPs under the action of ether oxygen chains, which eventually realize a t_{Li+} of 0.48. Different

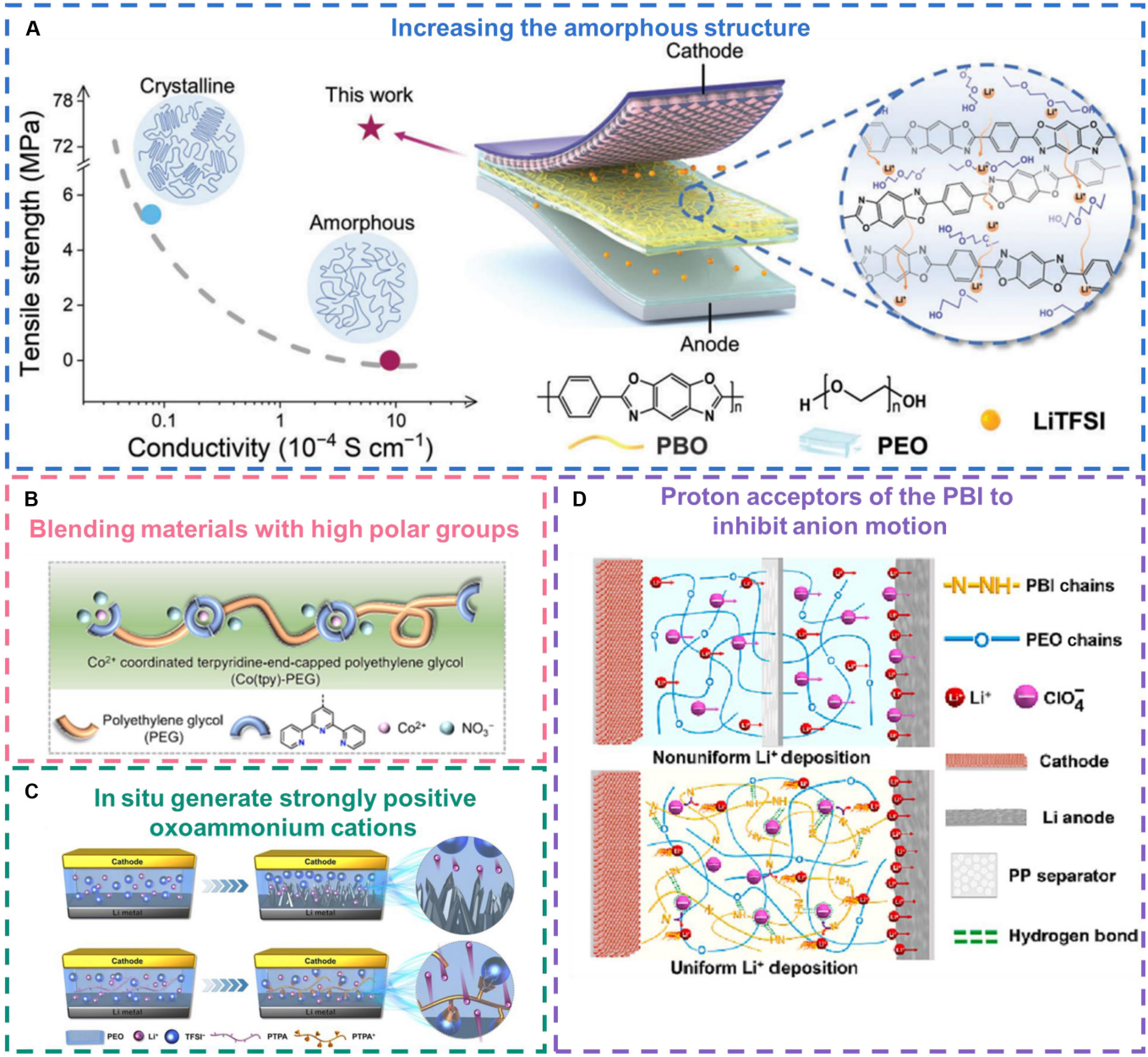


Fig. 6. (A) Diagram illustrating the trade-off between ionic conductivity and mechanical strength in PEO/PBO composite SPEs [116]. Adapted with permission of [116]. Copyright 2024, Wiley-VCH GmbH. (B) Diagram illustrating elements of Co(tpy)-PEG [126]. Adapted with permission of [126]. Copyright 2024, Elsevier B.V. (C) Diagram illustrating the function of PTPA on various PEO-based electrolytes (the above of diagram is cells without PTPA and the bottom of that is cells with PTPA) [135]. Adapted with permission of [135]. Copyright 2025, Elsevier B.V. (D) Schematic diagram of Li^+ transport and Li^+ deposition behaviors on Li anode surface for the effect of lithium dendrite formation with and without PBI [138]. Adapted with permission of [138]. Copyright 2023, Elsevier B.V.

from them, Duan et al. [136] innovatively employed oxygen vacancies to assist in anchoring anions. The positively charged oxygen vacancies of Ov-CeO_2 can effectively increase the Lewis acidity of the PVDF-HFP/Ov-CeO_2 nanostructured framework, which interacts with the $TFSI^-$ and the ether oxygen bonding in the PEO, thus facilitating the mobility of Li^+. Zou et al. [138] prepared PBI-reinforced PEO-based SPEs by blending PBI, $LiClO_4$, and PEO via a solution casting method to form a flexible, self-supporting PBI-PEO-2Li electrolyte (Fig. 6D). The proton acceptors (-N=) on the imidazole rings of the PBI segments form hydrogen bonds with anions to inhibit their motion, which achieved a conductivity of 5.7×10^{-4} S/cm and a high t_{Li+} of 0.639.

Furthermore, employing porous frameworks or introducing porous additives into the matrix to disrupt the ordered interface of PEO can also effectively suppress crystallinity. High-porosity porous polymer scaffolds substantially enlarge the interfacial area with the PEO matrix, thereby disrupting the local chain ordering and crystalline packing of PEO. Generally, the smaller pore size of the polymer framework indicates higher ionic conductivity. Moreover, molecular dynamics simulations have demonstrated that nanoscale confinement can accelerate the diffusional motion of molecules in SPEs [140], yet this acceleration is counterbalanced when the confining channel is reduced to approximately 2 nm, where the enhanced ion–ion association markedly decreases the population of free charge carriers

so that the ionic conductivity does not exhibit a commensurate increase despite the facilitated local dynamics. Poly(2,2,6,6-tetramethylpiperidin-4-yl methacrylate)-wrapped hollow porous SiO_2 nanospheres were incorporated to create a tailored interface area between surface-modified inorganic filler particles and PEO materials, inhibiting PEO matrix crystallization and establishing rapid Li^+ transport channels (1.3×10^{-4} S/cm at 25 °C) [141]. Inspired by gas foaming technology employed in the polymer porous scaffold field, Li et al. [142] prepared porous PEO-based electrolytes via solvothermal methods. The pore structure obtained via solvent boiling can suppress crystallization of the PEO chain segment and reduce the density of electrolytes, demonstrating the effectiveness in enhancing the ionic conductivity by regulating the PEO interface area.

Besides, the self-supporting ultrathin polymer electrolyte with superior mechanical performance offers another avenue for optimizing ionic conductivity. By reducing the electrolyte thickness, the ion transport pathways are greatly shortened and the volume rate of electrolytes on cells is reduced, thereby accelerating overall ion transport and improving overall portability [143]. This means that more scale-up scope and application, including flexible conformability for wearable devices or higher energy density for storage systems, can be realized. Although harsher requirements were proposed for ultrathin SPEs than conditional SPEs, several methods were developed to further realize the ultrathin SPE-based cells. Liu et al. [144] developed an ultrathin aramid nanofiber (ANF)/PEO-LiTFSI SPE through a novel vacuum filtration method followed by a drying process. Compared to the traditional solution-casted PEO-LiTFSI electrolyte (187 μm), this ANF/PEO-LiTFSI electrolyte fabricated by vacuum filtration features a drastically reduced thickness of 23 μm and forms 3D continuous frameworks without aggregation, delivering a high ionic conductivity of 1.65 mS/cm and exhibiting another strategy to improve electrochemical performance of PEO-based SPEs. Due to insufficient thickness, ultrathin polymer electrolytes still require stringent mechanical properties to achieve self-supporting and molding. Introducing a 3D continuous network to enhance the mechanical properties of electrolytes is an effective way to achieve ultrathin SPEs, such as PVDF-HFP, PTFE, or PE matrix [145–149]. Representative polymer frameworks produced by electrospinning technology exhibits a remarkable role of providing a mechanical support for ultrathin SPEs. Ma et al. [145] employed PAN electrospun film as the matrix, which was filled with PEO and lithium salt ion conductors [lithium bis(trifluoromethanesulfonyl)imide]. The ultrathin SPE with a thickness of 5 μm was successfully prepared, where the unique interface, as well as the good mechanical strength, inhibits lithium dendrites and prevents short circuiting.

Electrochemical Window of Solid Polymer Electrolyte

Beyond the constraints of sluggish ionic conductivity, unmodified PEO chains typically possess terminal hydroxyl groups (-OH), which render PEO electrolytes highly susceptible to oxidative decomposition at high voltages and unstable at the anode interface. The hydrogen atoms on these end groups are highly reactive and serve as initiation sites for detrimental side reactions in the electrochemical environment. Under high-voltage oxidative environments (typically >3.9 V versus Li/Li^+), these terminal hydroxyls are highly prone to losing protons and electrons, undergoing oxidative dehydrogenation to generate highly reactive radical species. Rather than merely decaying, these radicals relentlessly attack C–H or C–O bonds along the polymer backbone. This catastrophic degradation culminates in deleterious gas evolution and a drastic surge in interfacial impedance, fundamentally restricting the anodic stability electrochemical window of the electrolyte.

Therefore, end-group modification, including methylation (forming $-OCH_3$) or acylation, serves as a primary method for enhancing the stability of PEO-based electrolytes. For instance, Shao et al. [150] reported 2 novel PEO polymers capped with terminal phenyl (PEO-P) and perfluorophenyl (PEO-FP) groups, synthesized by reacting the terminal hydroxyls of traditional PEO-OH with benzoyl chloride and 2,3,4,5,6-pentafluorobenzoyl chloride, respectively. The results showed that PEO with non-active benzene or pentafluorobenzene end groups exhibited relative stability, expanding the electrochemical window up to 5.2 V (Fig. 7A). The perfluorophenyl group covalently anchors 5 fluorine atoms at the polymer chain end, creating a concentrated electron-withdrawing field and physical barrier, which effectively lowers the highest occupied molecular orbital (HOMO) level, protects the terminal oxygen atoms, and promotes the formation of a dense LiF interfacial layer. In a similar vein, Shen et al. [24] developed a modified PEO featuring semi-ionic C–F (SIF) bonds, which substantially improved electrochemical stability under high voltages and raising the electrochemical window of SIF-PEO-based SPEs from 4.0 V to 4.5 V (Fig. 7B). The LMBs assembled with $LiNi_{0.5}Co_{0.2}Mn_{0.3}O_2$ demonstrated high cycling stability at 40 °C (99.79% Coulombic efficiency over 500 cycles at 0.5 C). This work confirms that the strong coordination between ether oxygen atoms and Li^+ on the traditional PEO chain can be effectively weakened through introduction of semi-ionic C–F bonds featuring electrostatic interactions with HOMO-lowering capability.

Furthermore, the generation of unfavorable by-products at the anode interface is also a major reason for poor electrochemical stability. Uncapped hydroxyl groups undergo irreversible redox reactions upon contact with lithium metal, thereby generating hydrogen gas and lithium salts with poor ionic conductivity (e.g., LiOH or lithium alkoxides). This parasitic interfacial reaction not only consumes active Li^+ but also forms an uneven, high-impedance SEI on the anode surface, hindering ion transport and inducing nonuniform dendrite growth. To address interfacial issues at the anode, Huang et al. [151] developed composite SPEs by combining PTFE porous membranes with PEO, lithium salts (LiTFSI and LiODFB), and PVDF-HFP (Fig. 7C). The PTFE host–solvent interaction greatly suppresses the activity of free solvent toward lithium anode. Instead, the $ODFB^-$ anion in LiODFB possesses superior oxidative stability and preferentially decomposes on the lithium metal anode surface to form a stable SEI layer rich in LiF and B–O compounds, further mitigating side reactions and enhancing electrolyte stability. Xie and Shi [152] designed a dual-solvent PEO-based SPEs, where tetraethylene glycol dimethyl ether (TEGDME) molecules establish a robust UV-cured cross-linked network with PEO (Fig. 7D) while succinonitrile (SN) small molecules engage in strong hydrogen bonding interactions with PEO, integrating LiODFB as an additive. Functioning as plasticizers, TEGDME and SN exhibit exceptional compatibility toward both the Li anode and $LiNi_{0.6}Mn_{0.2}Co_{0.2}O_2$ (NCM622) cathode, thus optimizing the electrolyte–electrode interface stability and achieving a high electrochemical window of 5.2 V. The corresponding

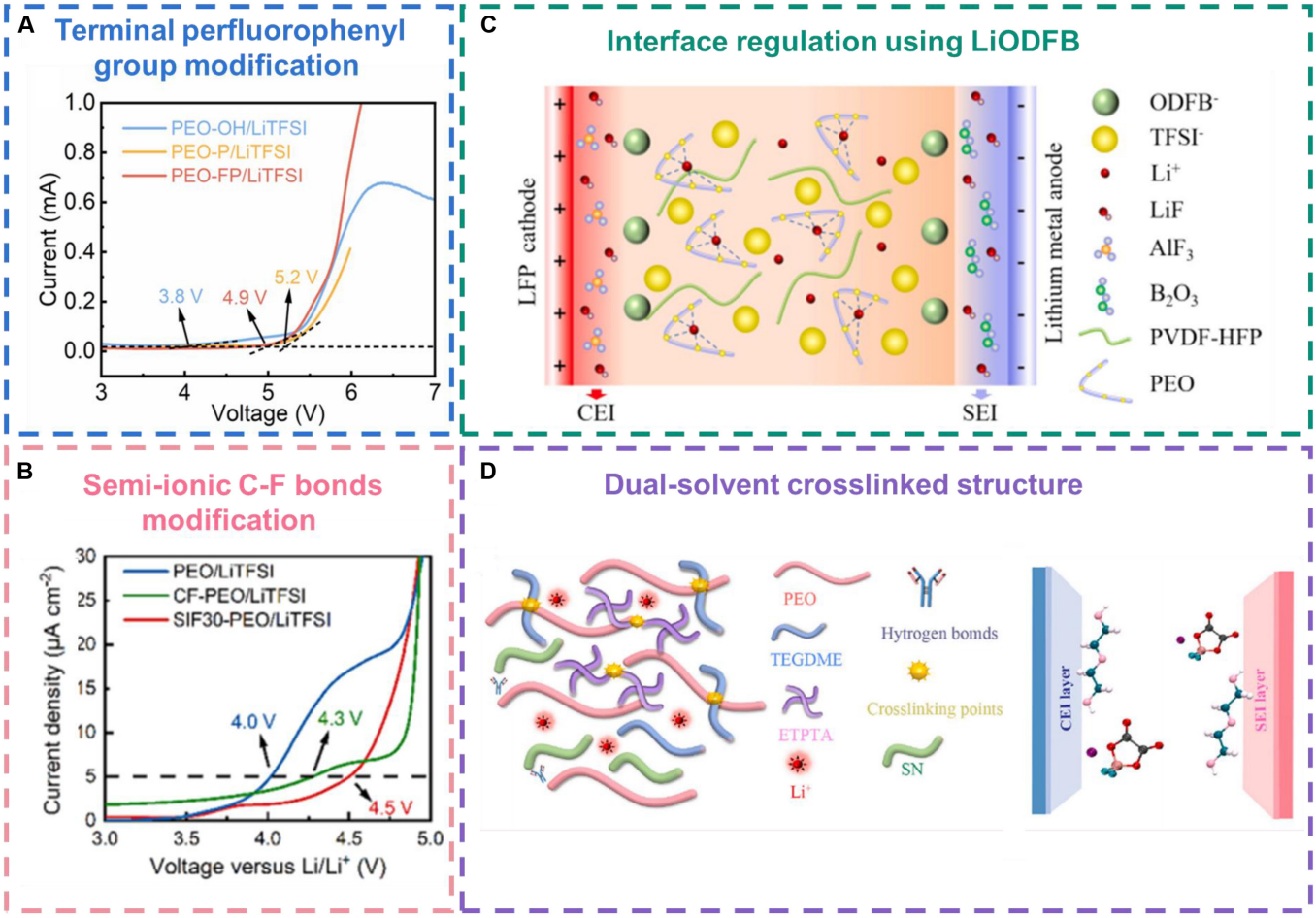


Fig. 7. (A) Electrochemical windows of PEO with different terminals [150]. Adapted with permission of [150]. Copyright 2025, American Chemical Society. (B) Electrochemical windows of PEO/LiTFSI, CF-PEO/LiTFSI, and SIF30-PEO/LiTFSI [24]. Adapted with permission of [24]. Copyright 2024, Elsevier B.V. (C) Diagram illustrating that the function of dual lithium salts enhanced composite PEO/PTFE SPEs [151]. Adapted with permission of [151]. Copyright 2025, Elsevier B.V. (D) Schematic illustration of the polymer chains interconnecting and generation of SEI and CEI layer for the dual-solvent PEO-based polymer electrolyte [152]. Adapted with permission of [152]. Copyright 2023, Elsevier B.V.

high-cathode-loading NCM622 cells (10 mg/cm^2) have a high-capacity retention of 86.6% after 100 cycles, with great potential in practical application.

In summary, the end capping strategy expands the electrochemical window by replacing the active hydroxyl group at the PEO chain end with a strong electron withdrawing group, lowering the HOMO energy level and blocking the oxidative decomposition pathway. Furthermore, the interface engineering strategy constructs a stable electrode/electrolyte interface by prioritizing the decomposition of salt or small molecule plasticizers into a film, further suppressing parasitic reactions and enhancing high-voltage cycling stability. Therefore, both the end-group chemistry and interface engineering exhibit the promising potential in improving the electrochemical window, confirming the effectiveness of polymer design strategies in high-voltage LMBs, which are considered as one of the essential pathways to overcome the high-voltage limitation of PEO-based electrolytes.

Operation Safety of Solid Polymer Electrolyte

The mechanical integrity of both solid electrolytes and separators serves as the primary physical barrier against lithium dendrite penetration. According to the Monroe–Newman theoretical criterion, the shear modulus of the electrolyte must reach approximately twice that of lithium metal (≈7 GPa) to effectively suppress dendrites [153]. However, the actual shear modulus of linear PEO at operating temperatures is merely on the order of MPa, far below this threshold. Therefore, SPEs with high modulus and superior puncture resistance can effectively suppress dendrite growth at the interface, ensuring excellent cycling stability and operational safety. Current research primarily employs polymer chain engineering strategies to enhance mechanical properties: (a) introducing rigid segments into flexible PEO chains via copolymerization or blending, utilizing microphase separation to form physical crosslinking domains that synergistically optimize mechanical rigidity and ionic conduction [154], and (b) constructing rigid frameworks such as porous skeletons, 3D crosslinked networks, or semi-interpenetrating networks, with PEO serving as the ion-conducting phase and the reinforcing framework as the mechanical support phase, achieving high modulus and exceptional dimensional stability [155]. Polymer electrolytes prepared via these methods typically exhibit excellent mechanical performance and dimensional stability [155–157].

Various reinforcing materials have been reported, including polyamide 6 (PA_6) [158,159] and polymers of intrinsic microporosity (PIMs) [154]. To improve the mechanical properties

of SPEs, Cao et al. [160] introduced hard PA_6 segments into the soft PEO matrix, where the hard PA_6 domains act as physical crosslinking points, thereby maintaining robust mechanical strength, while the soft PEO blocks provide ionic conduction pathways. Furthermore, the abundant amide groups in the PA_6 chains form reversible supramolecular hydrogen bonds, endowing the material with excellent self-healing capability. Fillers not only compensate for the intrinsic softness of flexible PEO but also disrupt its regular crystallinity, achieving simultaneous enhancement of both electrochemical and mechanical performance. Hu and Zhang [154] designed a PEO-based SPEs, with the rigid skeleton of PIM-1 as the hard segments, PEG as the soft segments, and 4,4′-diphenylmethane diisocyanate as the binder. Due to existing excellent mechanical properties of polyurethane hard segments, the high hard skeleton of PIM-1, and the strong hydrogen bonding interactions between polar functional groups (N–H and C=O) and PEO matrix, the designed SPEs have a much shallower displacement under the same pressing force than pure PEO-based SPEs, illustrating that superior mechanical strength tends to restrain the growth of lithium dendrites.

Moreover, the 3D cross-linked network typically serves as a filling skeleton for PEO-based electrolytes, effectively enhancing the mechanical property and capability of resisting the dendritic lithium, including electrospun PAN membranes [161] and cellulose membranes [162], which can enhance their mechanical strength and resisting puncture by lithium dendrites. For instance, Liang et al. [148] impregnated PEO/LiTFSI electrolyte into a porous PTFE matrix through a strategic combination of blade-coating and hot-pressing processes (Fig. 8A). The form thickness of the resulting ultrathin composite polymer electrolyte decreased to 6 μm via hot-pressing processes, achieving excellent mechanical properties due to the reinforcing effect of the PTFE matrix (Fig. 8B). The corresponding LFP cells (cathode loading = 7.64 mg/cm^2) exhibit a quite stable charge–discharge process during cycling. Notably, Sarmad et al. [161] dispersed $Li_{6.3}La_3Zr_{1.4}Ta_{0.6}O_{12}$ particles on the PAN nanofiber membrane using electrospinning, followed by infiltrating a PEO/LiTFSI polymer matrix into the scaffold. The tensile strength of the PEO-PAN electrolyte was appreciably enhanced (5.2 MPa) than that of pure PEO (1.5 MPa). Crucially, the 3D structure of the electrospun PAN membrane acts as a robust physical barrier, effectively blocking dendrite growth and preventing internal short circuits in the battery. However, insufficient adhesion between the skeleton and PEO can lead to increased interfacial voids, hindering ion transport and increasing interfacial resistance. If the content of the skeleton is too low, the enhancement effect is limited. If it is too high, it can lead to a decrease in ionic conductivity. Moreover, in an electrochemical-temperature-mechanical multiphysics field model, Zhang et al. [163] identified that the anisotropy of the bulk membrane will influence the dendrite growth. When the anisotropy strength increases, the growth rate of the dendritic main branch similarly increases progressively. Therefore, the precise design of PEO-based polymer skeletons is also one of the main directions that need to be explored in the future.

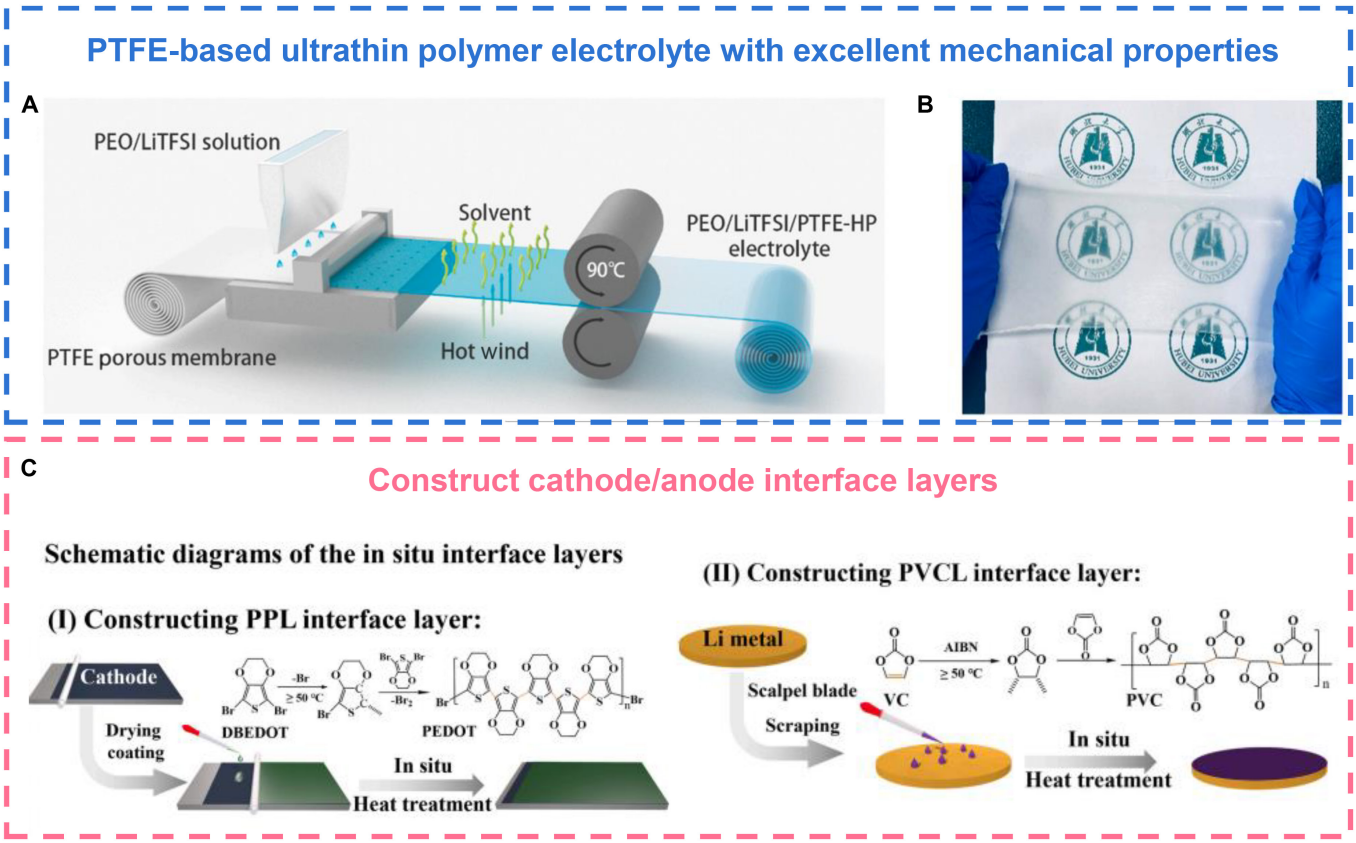


Fig. 8. (A) Schematic diagram of preparation process for porous PTFE-based composite polymer electrolytes and (B) its photograph [148]. Adapted with permission of [148]. Copyright 2023, Elsevier B.V. (C) Schematic illustrating the construction strategy of SPEs for both interface layers [164]. Adapted with permission of [164]. Copyright 2023, Elsevier B.V.

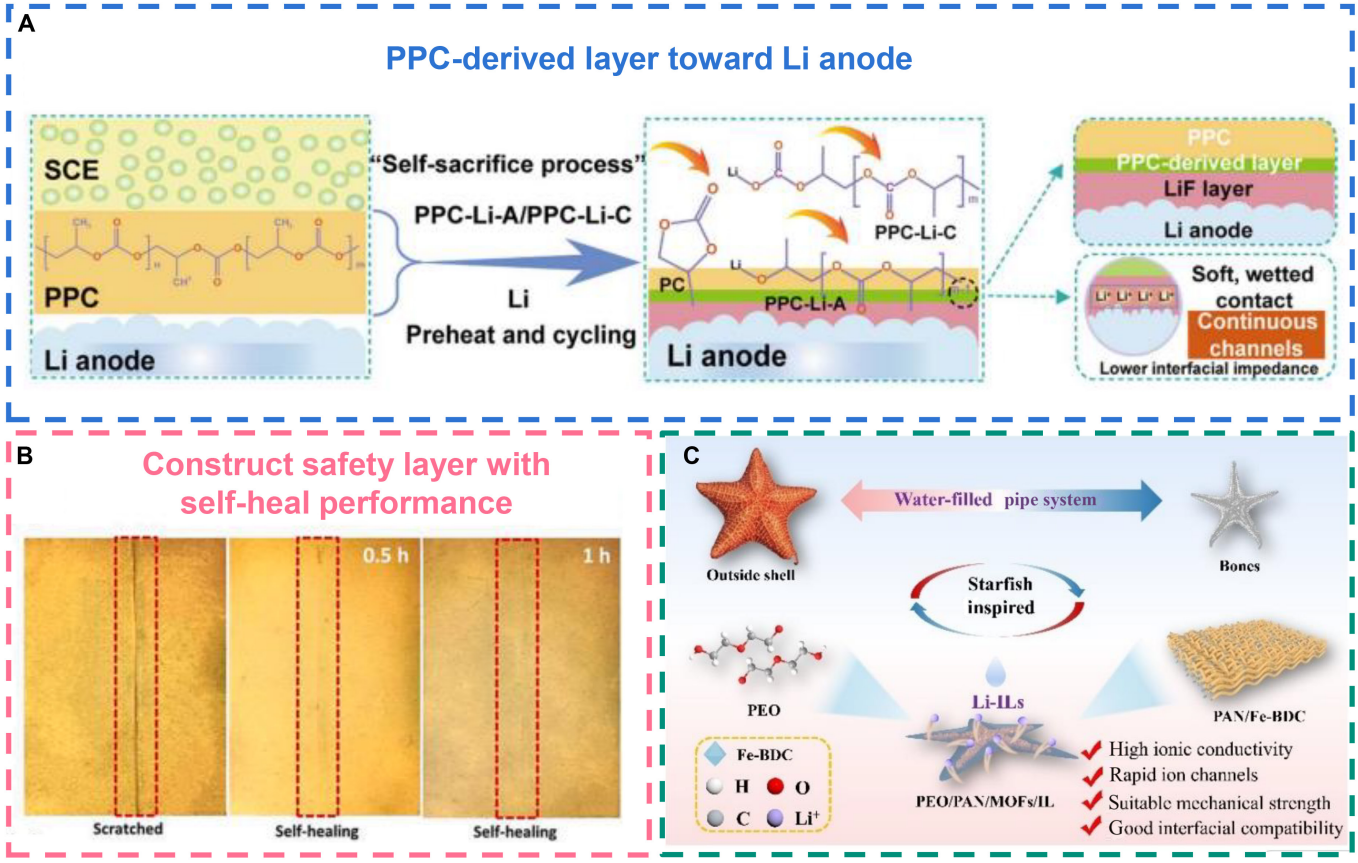


Fig. 9 (A) Schematic illustrating the PPC "self-sacrifice" process [5]. Adapted with permission of [5]. Copyright 2024, Royal Society of Chemistry. (B) Digital photos illustrating the self-heal performance of PPC-based SPEs [168]. Adapted with permission of [168]. Copyright 2024, Royal Society of Chemistry. (C) Schematic illustrating the starfish-inspired SPEs and the multifunctional synergistic mechanisms of the PEO/PAN/MOFs/ionic liquid film [174]. Adapted with permission of [174]. Copyright 2025, Wiley-VCH GmbH.

Moreover, the interface stability and long-term performance are critical prerequisites for ensuring the operational safety of solid-state LMBs. As a component directly contacting with electrode, SPEs themselves can introduce element or interfacial layers to improve the solvation structure or interfacial reactions, thereby tailoring the interface toward the high-voltage cathode and the high-reactivity anode. Currently, it is known that a robust and uniform SEI is key to increase the lifespan of LMBs. Therefore, precise polymer design strategies for manipulating SEI element are constantly explored. For example, Zheng et al. [164] constructed an asymmetric interfacial layer comprising poly(3,4-ethylenedioxythiophene) facing the cathode and poly(vinyl carbonate) facing the anode (Fig. 8C), yielding stable fast-ion conduction characteristics, with LiF, Li_3N, and LiBr enriching the lithium metal surface after cycling. This dual-interface strategy provides a reliable pathway to overcome interfacial bottlenecks in solid-state lithium batteries. On the other hand, the detailed mechanism of charge transfer behavior on the formation of SEI is also discovered through the rational polymer design. Liang et al. [165] constructed a porous organic polymer with "charge storage" properties and doped into a polymer composite solid electrolyte to further study the effect of sufficient charge transfer on the decomposition of lithium salts. Further, the LiTFSI decomposition mechanism about the charge transfer process was concluded comprehensively by using charge density difference calculations and AIMD simulation time:

$$LiN(SO_2CF_3)_2 + e^- = CF_3^- + SO_2^- + LiNSO_2CF_3^- \quad (3)$$

$$LiNSO_2CF_3^- + e^- = CF_3^- + LiNSO_2^- \quad (4)$$

$$CF_3^- + e^- = CF_2^- + F^- \quad (5)$$

$$Li^+ + F^- = LiF \quad (6)$$

AIMD simulations reveal that SEI formation is governed by a distinct 4-stage pathway induced by consecutive charge transfer. The process initiates with the reductive cleavage of LiTFSI into CF_3^-, SO_2^-, and $LiNSO_2CF_3^-$ intermediates, followed by the subsequent reduction of $LiNSO_2CF_3^-$ into $LiNSO_2^-$. The generated CF_3^- fragments then undergo further electron-driven defluorination to liberate F^- ions. Ultimately, the reaction concludes with the combination of Li^+ and F^- to precipitate LiF, thereby driving the phase evolution and structural development of the inorganic SEI layer. Specifically, in the bulk electrolyte, the solvation structure of LiTFSI is influenced by the coordination between polymer chains and Li^+, as well as the electrostatic interaction between $TFSI^-$ and Li^+, which usually exists in the form of CIPs and AGGs. The $TFSI^-$ anions are anchored by the delocalized skeleton via strong electrostatic/Lewis acid-base interactions, which simultaneously weaken the C–S and S–N bonds and extend the Li^+–$TFSI^-$ distance, facilitating the CIP-to-SSIP transition and lowering the lowest unoccupied molecular orbital energy to a pre-polarized state. Upon Li^+ desolvation at the electrode, the anion's immobility limited

Table 2. Summary of the performance comparison between PEO-based SPEs

References	Sample	Polymer	t_{Li+}	Ionic conductivity (mS/cm)	Tensile strength (MPa)	Electrochemical window (vs. Li/Li$^+$)
[116]	PBO/PEO	PEO, PBO	N/A	0.61 (60 °C)	74.4	4.6 V
[117]	PEO/LiTFSI	PEO	0.31	≈0.47 (70 °C)	N/A	N/A
[126]	CPE-PEO/Co(tpy)-PEG	PEO, PEG	0.75	0.22 (60 °C)	>0.9	5.2 V
[135]	PPL	PEO, PTPA	0.57	0.76 (60 °C)	1.05	5.0 V
[137]	CbzTM@C9	PEO	0.48	0.8 (60 °C)	1.26	≈6.3 V
[136]	Ov-CeO_2-CSE	PEO, PVDF-HFP	0.49	0.176 (30 °C)	7.34	>5.3 V
[138]	PBI-PEO-2Li	PBI, PEO	0.639	0.57 (25 °C)	5.27	4.45 V
[141]	7.5%P@ SiO_2@P-PEO-1/8LiClO4	PEO, PTMPM	0.81	0.13 (20 °C)	N/A	>5 V
[142]	B-PEO/SN/LLZTO	PEO	0.26	0.226 (25 °C)	N/A	N/A
[144]	5ANF25Li	PEO	N/A	0.155 (30 °C)	2.59	4.5 V
[145]	PAN-PEO/LiTFSI	PAN, PEO	N/A	N/A	~0.01	N/A
[150]	PEO-FP/LiTFSI	Perfluorophenyl-terminated PEO	0.49	N/A	N/A	4.9 V
[24]	SIF30-PEO/LiTFSI	Semi-ionic C–F modified PEO	N/A	0.076 (40 °C)	N/A	4.5 V
[151]	CSE-2	PEO, PVDF-HFP, PTFE	0.42	N/A	4.38	5.1 V
[152]	DSPE	PEO	0.79	0.57 (30 °C)	≈1.7	4.6 V
[178]	V-SPE-PEG	PEO, PEGDME	0.33 (60 °C)	0.27 (30 °C)	3.16	4.61 V
[154]	CPE-15% PPU	PIMs, PEG, PEO, polyurethanes	0.68	1.82 (50 °C)	4.1	5.3 V
[148]	PLP-HP	PEO, PTFE	N/A	N/A	63	N/A
[161]	PEO-PAN/LLZTO-8%	PEO, PAN	N/A	0.065 (30 °C)	7.2	5.0 V
[164]	PPL-PEO-PVCL	PEO, PVC, PEDOT, PPL	0.47	0.1025 (25 °C)	N/A	4.6 V
[165]	PEO-POF-1 wt %	PEO, porphyrin-based POF	0.64	0.284	N/A	4.61 V
[166]	CSE-4-FP	Porous organic polymers, PEO	0.155	N/A	N/A	5.0 V
[5]	PEO-SCE-PPC	PEO, PPC	N/A	0.321 (30 °C)	N/A	N/A
[168]	PIBCPE_27	PIL-containing triblock copolymer, PVDF-HFP	0.57	0.37 (25 °C)	5.39	5.0 V
[174]	FAEI	PAN, PEO	0.69	0.437 (25 °C)	29.1	5.34 V

by the polymer results in its interfacial enrichment, thus forming an anion-dense double layer that acts as a substantial feedstock for reductive decomposition. It identified that a porous organic polymer with "charge storage" properties allows LiTFSI to gain enough charge and promotes the dissociation of LiTFSI to take shape a LiF-rich SEI. Impressively, Zhou et al. [166] further optimized SEI components by tailoring the fluorine substitution sites on the benzene rings of porous organic polymers to control LiF concentration in the SEI. The battery exhibited optimal performance when the LiF content was approximately 8.7%. This work provides a crucial strategy for enhancing the performance of PEO-based all-solid-state LMBs via the polymer design and SEI composition control.

Beyond mechanical and electrochemical stability, the rational polymer design can endow PEO-based SPEs with additional safety-critical functionalities. The exceptional structural versatility of polymers and the multifunctionality of different polymers have endowed SPEs with diversified development routes [167]. Wang et al. [5] proposed an asymmetrical multilayered composite electrolyte design, where a highly flexible PEO buffer

layer is positioned against the cathode, while the PPC polymer contacts the anode, effectively minimizing interfacial resistance (Fig. 9A). PEO plays a vital role of contacting with the cathode, while PPC renders decreased interface resistance. The asymmetrical multifunctional design provides the polymer more pathway to improve the existing problem. Gao et al. [168] employed highly reversible ion–dipole interactions to endow composite solid electrolytes with excellent self-healing performance at room temperature (Fig. 9B), with dual ion–dipole interactions between the imidazolium cations in poly(ionic liquid)s blocks and the alkoxy dipoles in PEO and the -CF_3 dipoles in PVDF-HFP. The high reversibility of ion–dipole interactions endowed SPEs outstanding self-healing property without any external stimulation at ambient temperature. Beyond the dual ion–dipole interactions, a range of physicochemical strategies have been exploited to confer self-healing capability on SPEs, including dynamic imine networks formed via Schiff base reactions [169], in situ alloying with liquid metal [170], reversible imine and disulfide bonds [171], semi-interpenetrating networks based on Diels–Alder dynamic crosslinking [172], and the interaction between 3D amorphous carbon and the PEO matrix [173]. Self-healing electrolytes can repair damage induced by dendrite penetration or mechanical fatigue during cycling, maintaining mechanical integrity and interfacial stability. Additionally, researchers have developed multifunctional "starfish-type" composite polymer electrolytes (PAN/MOFs/ionic liquids). Here, rigid MOF cores are enveloped by a PEO buffering layer to ensure electrode compatibility, while ionic liquids are incorporated in the PAN matrix to minimize interfacial resistance, culminating in a synergy of mechanical and electrochemical enhancements (Fig. 9C) [174].

In summary, through various means such as polymer frameworks and rigid polymer fillers, synchronous enhancement of the mechanical and electrochemical stability of SPEs can be achieved. In addition, the reasonable polymer design, including various groups or multifunctional polymers, endows solid electrolytes based on PEO with safety-critical functions in addition to mechanical and electrochemical stability. These strategies highlight the multifunctionality of polymer engineering in developing advanced and safe PEO-based electrolytes (Table 2) [175,176].

Conclusion and Perspectives

This review comprehensively discussed recent advancement of polymer design strategy for LMBs, focusing on its application in separators and SPEs. By concluding various methods, functionalized separators and SPEs have demonstrated remarkable effectiveness of the polymer design strategy to accelerate Li^+ transport and inhibit lithium dendrite growth. However, separators possess mature processing technology but rely on flammable liquid electrolytes and face thermal shrinkage and dendrite penetration risks. SPEs provide intrinsic safety and good interfacial compatibility with lithium metal, yet are constrained by low room-temperature conductivity, modest mechanical properties, and narrow electrochemical windows. The reinforcement in safety is critical for separator engineering whereas the electrochemical performance is lacking for SPEs. In the long term, separators and SPEs should be understood as 2 ends of a single technological spectrum rather than isolated domains. Separators and SPEs are capable of both physical separation and ion transport; thereby, bulk electron-blocking and ion-conducting are the foundations of polymer design strategies. Based on this principle, developing high-performance polymer separator and SPEs via elaborated polymer design strategies can further facilitate the advancement of high-safety LMBs.

Although the polymer design strategy shows great potential in developing the advanced separator or SPEs, the transition from laboratory breakthroughs to practical commercialization faces substantial hinders: First, most experiments merely provide simple verification of the effects of modification methods on electrochemical performance, without delving into the precise experimental design to explore the underlying mechanisms and elucidate specific structure–performance relationships, which provides vague guidance rather than clear inspiration for future researchers in this field. Second, although the SPEs have realized improvements in electrochemical window, their compatibility with next-generation high-voltage cathodes and high-loading anodes still requires further enhancement to compete with liquid counterparts in energy density. Additionally, the mechanical conflict between the rigidity required for dendrite suppression and the flexibility needed for interfacial contact is still a trade-off that single material systems struggle to resolve completely.

Advancements in elaborated polymer design strategies for LMBs can be directed toward comprehensive integration and precise design principles. Research should not merely focus on optimizing a single property, but should concentrate on developing multifunctional systems, including multi-functional, multi-layer polymer designs or architectures, thereby meeting various requirements posed by both cathode and anode materials. The trajectory points toward integrated ion-conducting membranes that combine mechanical support, ion transport, and interfacial regulation within a unified architecture. Furthermore, the precise experimental design and in-depth mechanism study can help elucidate the intrinsic pathway to enhance the performance and safety of LMBs. Combining the function-oriented precise integration design with the ever-growing demand can overcome current limitations and pave the way for safe, high-energy-density energy storage solutions via innovative polymer design strategies.

Acknowledgments

Funding: This work was supported by the National Natural Science Foundation of China (52373211 and 52622312) and the Fundamental Research Funds for the Central Universities (2232019A3-03).
Competing interests: The authors declare that they have no competing interests.
AI tool usage declaration: The schematic diagram insets in Fig. 1 are generated by AI and modified by the authors.

References

1. Niu H, Zhang N, Lu Y, Zhang Z, Li M, Liu J, Zhang N, Song W, Zhao Y, Miao Z. Strategies toward the development of high-energy-density lithium batteries. *J Energy Storage*. 2024;88:Article 111666.
2. Liu J, Zhang YH, Zhou JQ, Wang ZK, Zhu P, Cao YF, Zheng YW, Zhou X, Yan CL, Qian T. Advances and prospects in improving the utilization efficiency of lithium for high energy density lithium batteries. *Adv Funct Mater*. 2023;33(34):2302055.

3. Fan W, Miao YE, Zhang LS, Huang YP, Liu TX. Porous graphene–carbon nanotube hybrid paper as a flexible nano-scaffold for polyaniline immobilization and application in all-solid-state supercapacitors. *RSC Adv*. 2015;5(39):31064–31073.
4. Zhang LS, Liao M, Bao LK, Sun XM, Peng HS. The functionalization of miniature energy-storage devices. *Small Methods*. 2017;1(9):1700211.
5. Wang Z, Tan JW, Cui JW, Xie KY, Bai YF, Jia ZH, Gao XW, Wu YP, Tang W. A novel asymmetrical multilayered composite electrolyte for high-performance ambient-temperature all-solid-state lithium batteries. *J Mater Chem A*. 2024;12(7):4231–4239.
6. Zhang LS, Fan W, Liu TX. A flexible free-standing defect-rich MoS_2/graphene/carbon nanotube hybrid paper as a binder-free anode for high-performance lithium ion batteries. *RSC Adv*. 2015;5(54):43130–43140.
7. Fu F, Jiao X, Yang Y, Yin X, Zheng ZJ. Wood-based materials for high-energy-density lithium metal batteries. *Nano Energy*. 2025;133:Article 110464.
8. Wang XS, Wu JR, Wang HR, Yin XS, Zhou Z, Huang YY, Zhang YL, Li WS, Li BH. Lithium nitrate effects for lithium-based chemical batteries: A review. *Carbon Energy*. 2026;8(1):Article e70090.
9. Jia WS, Zhang JF, Zheng LJ, Zhou H, Zou W, Wang LP. Lithium-rich alloy as stable lithium metal composite anode for lithium batteries. *Escience*. 2024;4(6):Article 100266.
10. Tao M, Chen J, Lin H, Zhou Y, Zhao D, Shan P, Jin Y, Yang Y. Recent advances in quantifying the inactive lithium and failure mechanism of Li anodes in rechargeable lithium metal batteries. *J Energy Chem*. 2024;96:226–248.
11. Bae J, Choi K, Cheong JY, Ahn S, Cho S, Im SG, Kim I-D. Emerging surface engineering methods for lithium metal anodes: Critical review beyond conventional sei and surface coatings. *Adv Mater*. 2025;37(38):2501959.
12. Zhou KJ, Wang Y, Mei JB, Zhang X, Xue TT, Fan W, Zhang LS, Liu TX, Xie Y. Scalable preparation of polyimide sandwiched separator for durable high-rate lithium-metal battery. *Small*. 2024;20(6):2305596.
13. Tang WM, Zhao T, Wang K, Yu TY, Lv RX, Li L, Wu F, Chen RJ. Dendrite-free lithium metal batteries enabled by coordination chemistry in polymer-ceramic modified separators. *Adv Funct Mater*. 2024;34(18):2314045.
14. Wang ZY, Xu HR, Liu KF, Dong NX, Jia NF, Liu BX, Lin DL, Zhao Z, Tian GF, Qi SL, et al. Separator engineering regulating reversible Li electrodeposition enabled by lithiophilic polyimide@ag coating layer for dendrite-free lithium metal batteries. *Small*. 2025;21(33):2504870.
15. Luo YJ, Zhang YY, Tan ZQ, Zhou KJ, Zhang LS, Liu TX. Design strategies of polyimide aerogel separators for rechargeable lithium batteries. *Batteries Supercaps*. 2026;9(7):Article e70388.
16. Babiker DMD, Usha ZR, Wan CX, Hassaan MME, Chen X, Li LB. Recent progress of composite polyethylene separators for lithium/ sodium batteries. *J Power Sources*. 2023;564:Article 232853.
17. Li XL, Li XW, Zhang LJ, Niu ZH, Wen GW. Research progress of alumina ultrafine powder modified lithium-ion battery separators. *Chem Eng J*. 2025;523:Article 168561.
18. Wang ZY, Zhao CZ, Yao N, Lu Y, Xue ZQ, Huang XY, Xu P, Huang WZ, Wang ZX, Huang JQ, et al. The regulation of solid electrolyte interphase on composite lithium anodes in solid-state batteries. *Angew Chem Int Ed*. 2025;64(2):Article e202414524.
19. Yin AN, Yang SS, Wang CZ, Zhao Y, Miao RQ, Lu CQ, Tang R, Fang DB, He JX, Zhang JH, et al. Dense and strong garnet-type solid electrolyte stabilizing lithium metal for solid-state lithium metal batteries. *Energy Storage Mater*. 2025;82:Article 104665.
20. Liu SJ, Zhou L, Zhong TJ, Wu X, Neyts K. Sulfide/polymer composite solid-state electrolytes for all-solid-state lithium batteries. *Adv Energy Mater*. 2024;14(48):2403602.
21. Guo C, Luo ZH, Zhou MX, Wu X, Shi Y, An Q, Shao JJ, Zhou G. Clay-originated two-dimensional holey silica separator for dendrite-free lithium metal anode. *Small*. 2023;19(34):2301428.
22. Fan Z, Chen X, Shi J, Nie H, Zhang X, Zhou X, Xie X, Xue Z. Functionalized separators boosting electrochemical performances for lithium batteries. *Nano Micro Lett*. 2025;17(1):128.
23. Dai Z, Su Y, Liu D, Han Q, Greaves TL, Lei W, Liu Z, Chen Z. Metal-organic frameworks based solid-state electrolytes for high-performance lithium metal batteries. *Chem Eng J*. 2025;524:Article 169365.
24. Shen JQ, Liu SH, Han XJ, Chen ZX, Tian WS, Yang C, Pan H, Chen SW, Zhu SM. Regulating the Li-O coordination in polymer electrolytes via semi-ionic C-F bonds for high-voltage solid lithium metal batteries. *Chem Eng J*. 2024;484:Article 149497.
25. Zhang MJ, Pal U, Makhlooghiazad F, O'Dell LA, Kondou S, Elia GA, Gerbaldi C, Forsyth M. Advanced high-voltage electrolyte design using poly(ethylene oxide) and high-concentration ionic liquids for all-solid-state lithium-metal batteries. *ACS Appl Mater Interfaces*. 2024;16(41):56095–56105.
26. Yang Y, Sun Z, Wu Y, Liang Z, Li F, Zhu M, Liu J. Porous organic framework materials (MOF, COF, and HOF) as the multifunctional separator for rechargeable lithium metal batteries. *Small*. 2024;20(37):2401457.
27. Duan S, Qian L, Zheng Y, Zhu Y, Liu X, Dong L, Yan W, Zhang J. Mechanisms of the accelerated Li^+ conduction in MOF-based solid-state polymer electrolytes for all-solid-state lithium metal batteries. *Adv Mater*. 2024;36(32):2314120.
28. Lin Z, Sheng O, Cai X, Duan D, Yue K, Nai J, Wang Y, Liu T, Tao X, Liu Y. Solid polymer electrolytes in all-solid-state lithium metal batteries: From microstructures to properties. *J Energy Chem*. 2023;81:358–378.
29. Cao L, Deng Y, Zhang S, Zhang B, Huang G, Wang J, Guo Z, Pan F. Separators for rechargeable metal batteries: Design principles and evaluation. *Adv Funct Mater*. 2025;35(30):2425517.
30. Ju Y, Kim B, Youn B, Song Y, Jang H, Lee D. Towards dendrite-free lithium-ion batteries: A comprehensive review of functional separator technologies. *J Energy Storage*. 2025;127:Article 116957.
31. Seo J, Im J, Kim M, Song D, Yoon S, Cho KY. Recent progress of advanced functional separators in lithium metal batteries. *Small*. 2024;20(33):2312132.
32. Deng JH, Xie JK, Zhang GQ, Yang XQ. Research progress of cross-linked fiber membranes for lithium-ion battery separators. *Chem Eng Sci*. 2023;280:Article 118970.
33. Jia H, Zeng C, Lim HS, Simmons A, Zhang Y, Weber MH, Engelhard MH, Gao P, Niu C, Xu Z, et al. Important role of ion flux regulated by separators in lithium metal batteries. *Adv Mater*. 2024;36(19):2311312.
34. Yuan YJ, Li Y, Hu JX, Zhang KY, Zhang SZ, Yang B, Yao YC. The advanced copper oxide coating separator enhances

the electrochemical performance of high-rate lithium-ion batteries. *J Power Sources*. 2024;623:Article 235412.
35. Yuan HY, Zhang YY, Gao Y, Ali S, Hong C, Tang GJ, Cui JY, Wang Y, Xu HY, Xu TT. Two-dimensional titania-assisted synthesis of flaky amorphous nano-alumina as a high-performance separator coating for lithium metal batteries. *J Colloid Interface Sci*. 2025;686:930–940.
36. He QP, Ding L, Li DD, Zhang YJ, Zhang SH. Effect of hydroxy-terminated hyperbranched polymer coated separator on the lithium-ion battery performances. *J Polym Eng*. 2024;44(7):437–448.
37. Dai XK, Yu FS, Wen JW, Wang CX, Ma XL, Yang W, Huang GY, Ye HM. Robust and high-wettability pristine poly(ether ether ketone) nanofiber separator for heat-resistant and safe lithium-ion battery. *Chin J Polym Sci*. 2023;41(12):1937–1946.
38. Wu YK, Wu Q, Sun MJ, Zeng ZQ, Cheng SJ, Xie J. Enhancing safety in lithium batteries: A review on functional separators controlling substance and heat during thermal runaway. *Adv Funct Mater*. 2025;35(30):2425698.
39. Zhang J, Liu Z, Dang C, Zhu X, Zhang T, Shen J, Yang H, Zhang Y, Cao Y, Yuan CY, et al. From lab to industry: High-safety separators for lithium-ion/-metal batteries. *Matter*. 2025;8(6):Article 102101.
40. Shen X, Li Y. Fluorinated engineering toward stable lithium metal batteries. *Nano Energy*. 2025;141:Article 111106.
41. Fan ZX, Shi Z, Meng JC, Liu D, Guo KR, Xue ZG. Multifunctional supramolecular elastomer-coated separator for high-rate and safe lithium metal batteries. *Chem Eng J*. 2025;522:Article 167388.
42. Chen JC, Zhu GS, Xu HR, Jiang KP, Zhao YY, Wang H, Bai YR, Liao MJ, Mo XF, Li XY. High ionic conductivity polymer modified commercial separator for lithium metal battery. *J Power Sources*. 2025;653:Article 237681.
43. Chen Y, Mickel P, Pei HJ, Wen YF, Guan X, Wang Y, Wang XY, Al Mhtachem O, Zhang C, Nie H, et al. Bioinspired separator with ion-selective nanochannels for lithium metal batteries. *ACS Appl Mater Interfaces*. 2023;15(14):18333–18342.
44. Li JB, Yin GJ, Wang YN, Xiang Y, Yu N, Li X, Jiang YZ, Xu MW, Zhang X. Enhancing the electrochemical performance and safety of lithium-ion battery fluorinated MOF-based multifunctional separator. *Chem Eng J*. 2025;507:Article 160148.
45. Ren HP, Wang B, Zhou R, Wu B, Yang SJ, Wei ZZ, Zhao Y. Fiber-based composite separator with stable interface and high ionic transport capacity for lithium batteries. *ACS Appl Mater Interfaces*. 2025;17(8):12610–12620.
46. Zhou Q, Hussain S, Huang H, Hu JS, Zhang WX, Zhang B, Wang L. Amino-rich polybenzimidazole-mediated interfacial engineering in OPBI/halloysite nanotube composite separators for enhanced lithium-ion battery performance. *Small*. 2025;21(35):2504514.
47. Zheng T, Zhang Y, Huang N, Zhang H. Electrolyte transport in lithium-ion battery systems with nanoporous polyethylene separators: Insights from molecular dynamics simulations. *Comput Mater Sci*. 2024;242:Article 113099.
48. Liang T, Qian ZX, Liu JJ, Wang ZP, Nie HR, Liu FQ, Sun YL, Qu MJ. Phenolphthalein-based polyether sulfone separator with multi-carbonyl induced uniform lithium deposition for high-performance lithium metal batteries. *Chem Eng J*. 2025;512:Article 162449.
49. Chen H, Ren B, Wang Y, Liu M, He H, Chai L, Jia J, Yang X, Chen J, Li B. The fabrication of high-performance α-Al_2O_3 coated pe separator for lithium-ion batteries based on multiple hydrogen bonds. *Electrochim Acta*. 2023;465:Article 142985.
50. Shi C, Dai J, Li C, Shen X, Peng L, Zhang P, Wu D, Sun D, Zhao J. A modified ceramic-coating separator with high-temperature stability for lithium-ion battery. *Polymers*. 2017;9(5):159.
51. Jung MG, Oh JH, Hyun DE, Kim YN, Han JY, Shin WH, Jeong KH, Lee DW, Kim S, Oh JM. Effect of separator coating layer thickness on thermal and electrochemical properties of lithium-ion secondary batteries. *J Korean Ceram Soc*. 2024;61(6):1112–1122.
52. Li SZ, Yang HQ, Geng MZ, Do HN, Peng C. Molecular-level anion and Li+ co-regulation by amphoteric polymer separator for high-rate stable lithium metal anode. *Nano Lett*. 2023;24(1):486–492.
53. Zheng S, Mo L, Chen K, Chen AL, Zhang X, Fan X, Lai F, Wei Q, Miao Y-E, Liu T, et al. Precise control of Li^+ directed transport via electronegative polymer brushes on polyolefin separators for dendrite-free lithium deposition. *Adv Funct Mater*. 2022;32(41):2201430.
54. Sun S, Wang J, Chen X, Ma Q, Wang Y, Yang K, Yao X, Yang Z, Liu J, Xu H, et al. Thermally stable and dendrite-resistant separators toward highly robust lithium metal batteries. *Adv Energy Mater*. 2022;12(41):2202206.
55. Lu Z, Sui F, Miao YE, Liu G, Li C, Dong W, Cui J, Liu T, Wu J, Yang C. Polyimide separators for rechargeable batteries. *J Energy Chem*. 2021;58:170–197.
56. An H, Guo J, Gao J, Zhong Y, Li Y, Wang Z. Structural evolution of biaxially oriented polypropylene films upon asynchronous stretching. *J Polym Sci*. 2024;62(17):3947–3958.
57. Wang H, Wu Z, Lu Y, Zhang H, Cheng G, Liu G, Bai Y. Understanding the pore structure evolution of polyethylene separator with dissipative particle dynamics simulation. *Polym Eng Sci*. 2024;64(2):518–533.
58. Wang C, Wang W, Qi H, Dai Y, Jiang S, Ding B, Wang X, Li C, Zeng J, Wu T, et al. Electrospinning and electrospun nanofibers: From academic research to industrial production. *Prog Mater Sci*. 2025;154:Article 101494.
59. Wang SM, Yu YC, Fu ST, Li HT, Huang JJ. Regulating the non-effective carriers transport for high-performance lithium metal batteries. *J Energy Chem*. 2024;92:132–141.
60. Muche ZB, Nikodimos Y, Chang CY, Merso SK, Tekaligne TM, Shitaw KN, Serbessa GG, Hagos TM, Taklu BW, Agnihotri T, et al. Integrating electrodes and PVDF-HFP/Kevlar nanofiber separator for multi-functions using electrospinning. *Chem Eng J*. 2025;505:Article 159493.
61. Muche ZB, Nikodimos Y, Tekaligne TM, Merso SK, Agnihotri T, Serbessa GG, Wu SH, Su WN, Hwang BJ. Thermally stable 3d cross-linked fluorinated polyimide/PVDF-HFP hybrid separator for lithium battery applications. *Chem Eng J*. 2023;476:Article 146400.
62. Zhao HJ, Zhao GD, Liu FQ, Lan FF, Zhou JJ, Li L. A dual-network structured poly (m-phenylene isophthalamide) nanofiber separator with $Li_{6.4}La_3Zr_{1.4}Ta_{0.6}O_{12}$ for dendrite-free and high-safety lithium-metal batteries. *Chem Eng J*. 2024;490:Article 151559.
63. Liao C, Li WQ, Han LF, Chu FK, Zou B, Qiu SL, Kan YC, Song L, Yan W, He XM, et al. Microcapsule modification

strategy empowering separator multifunctionality to enhance safety of lithium-metal batteries. *Small*. 2024;20(43):2404470.
64. Lee J, Yoon J, Oh SG. Core-shell nanofiber separator incorporated with pda-pei co-modified $Li_{0.33}La_{0.57}TiO_3$ nanowires prepared by co-axial electrospinning for dendrite-free lithium metal batteries. *Mater Today Energy*. 2024;45:Article 101672.
65. Anggreini D, Haidar AH, Hawari NH, Yoo CY, Song X, Baskoro F, Sumboja A. Suppressing dendrites with garnet–polyimide nanofiber separators for durable anode-free lithium metal batteries. *ACS Appl Energy Mater*. 2026;9(3):1658–1668.
66. Qian YS, Chen K, Feng ZX, Ouyang Y, Lan QQ, Zhang C, Feng W, Miao YE, Liu TX. A fluorinated-polyimide-based composite nanofibrous separator with homogenized pore size for wide-temperature lithium metal batteries. *Small Struct*. 2023;4(8):2200383.
67. Du Z, Yu C, Yang X, Zhou Z, Sun J, Ai W. Dual-functional separator with high Li^+ flux and cation-selective transport for dendrite-free lithium metal anodes. *ACS Sustain Chem Eng*. 2025;13(51):22153–22162.
68. Lin G, Meng T, Peng Y, Li P, Hu X. Janus-architectured lithium replenishment separators boosting longevity of anode-free lithium metal batteries. *Small Methods*. 2025;9(3):2401133.
69. Zhai Y, Wu Y, Sheng J, Liu H, Huang Z, Xiao Q, Li L. An open-pore mfi zeolite nanosheet-modified separator with Li-ion flux regulation for lithium-metal batteries. *Chem Commun*. 2024;60(3):324–327.
70. Gao KX, Luo JH, Li X, Fan K, Luo LB, Liu XY. Electrospun heterocycle aramid nanofiber separator with MOF-supported porous structure enabled excellent cycling stability for lithium metal batteries with high lifepo4 loading. *J Alloys Compd*. 2023;966:Article 171549.
71. Wang KX, Duan J, Chen X, Wang JA, Li JQ, Jiang LX, Yan W, Lyu W, Liao YZ. Nanofibrous covalent organic frameworks based hierarchical porous separators for fast-charging and thermally stable lithium metal batteries. *Adv Energy Mater*. 2024;14(25):2401146.
72. Lee J, Yoon J, Jeon M, Oh S-G. Aramid-based composite nanofiber separator coated with thermal conductive layer containing hexagonal boron nitride for stable lithium metal batteries from dendritic Li growth. *Chem Eng J*. 2025;510:Article 161692.
73. Song X, Huang W, Wang H, Lu YM, Xing J. Polyimide/metal–organic framework-5 separator with excellent electrolyte wettability and thermal stability for high performance lithium-ion battery. *ACS Appl Polym Mater*. 2025;7(10):6312–6325.
74. Ding L, Li D, Zhang S, Zhang S, Wang Z, Du F, Zhang P, Yang F. Constructing valid Li^+ fast-transfer channels on novel P(TPC@Lys-Li) separator to enable security, high energy density, and controllable Li dendrites for lithium-metal batteries. *Chem Eng J*. 2024;501:Article 157586.
75. Wang XY, Wen YF, Wang Y, Chen Y, Yang LW, Guo C, Nie H, Zhou XP, Xie XL. PVDF/lithiated sulfonated poly (ether ether ketone) blend coated PE separators for high-performance lithium metal batteries. *J Power Sources*. 2024;615:Article 235126.
76. Jana A, Woo SI, Vikrant KSN, García RE. Electrochemomechanics of lithium dendrite growth. *Energy Environ Sci*. 2019;12(12):3595–3607.
77. Buragohain M, Kunnikuruvan S. Unveiling the role of ion pairs in determining electrolyte stability and solid electrolyte interphase formation in lithium metal batteries. *ACS Appl Energy Mater*. 2025;8(20):15334–15347.
78. Li Y, Wang Y, Chen B, Lin Y, Zhang G, Avdeev M, Shi S. Proactive lithium dendrite regulation enabled by manipulating separator microstructure using high-fidelity phase-field simulation. *Adv Energy Mater*. 2025;15(24):2500503.
79. Li Y, Zhang G, Chen B, Zhao W, Sha L, Wang D, Yu J, Shi S. Understanding the separator pore size inhibition effect on lithium dendrite via phase-field simulations. *Chin Chem Lett*. 2022;33(6):3287–3290.
80. Wang Y, Zhou KJ, Cui L, Mei JB, Li SN, Li L, Fan W, Zhang LS, Liu TX. Ion transport regulation of polyimide separator for safe and durable Li-metal battery. *J Power Sources*. 2024;591:Article 233853.
81. Guo D, Mu LQ, Lin F, Liu GL. Mesoporous polyimide thin films as dendrite-suppressing separators for lithium-metal batteries. *ACS Nano*. 2023;18(1):155–163.
82. Sheng L, Wang Q, Liu X, Cui H, Wang X, Xu Y, Li Z, Wang L, Chen Z, Xu G-L, et al. Suppressing electrolyte-lithium metal reactivity via Li^+-desolvation in uniform nano-porous separator. *Nat Commun*. 2022;13(1):172.
83. Ding L, Yue X, Zhang X, Chen Y, Liu J, Shi Z, Wang Z, Yan X, Liang Z. A polyimine aerogel separator with electron cloud design to boost Li-ion transport for stable Li metal batteries. *Proc Natl Acad Sci USA*. 2023;120(51):Article e2314264120.
84. Che RQ, Cheng S, Huang C, Liu M, Chen ZA, Han J, Chen W, Zhang PC. Poly(vinylidene fluoride)-based Janus separators with an ultrathin conductive layer for suppressing lithium dendrite growth. *Chem Eng J*. 2025;509:Article 161238.
85. Zhou KJ, Bao MX, Fang YK, He P, Ren JG, Zong W, Zhang LS, Liu TX. Single-atom zirconium coordination polyimide aerogel as separator coating toward high-rate lithium metal battery. *Adv Funct Mater*. 2025;35(1):2411963.
86. Xiang H, Zhang F, Zou B, Hou Q, Cheng C, Lu M, Wang X, Ping W, Sun Y, Song X. High-performance lithium batteries achieved by electrospun MXene-enhanced cation-selective membranes. *J Membr Sci*. 2024;704:Article 122867.
87. Zhong J, Tong Y, Guo L, Zhang A, Xu Q, Qin Y. Cationic covalent organic framework-modified polypropylene separator for high-performance lithium metal batteries. *ACS Appl Mater Interfaces*. 2024;16(41):56106–56115.
88. Jalees S, Hussain A, Iqbal R, Raza W, Ahmad A, Saleem A, Majeed MK, Faheem M, Ahmad N, Ur Rehman LN, et al. Functional PBI membrane based on polyimide covalent organic framework for durable lithium metal battery. *J Energy Storage*. 2024;101:Article 113985.
89. Zhou P, Zhang X, Xiang Y, Liu K. Strategies to enhance Li^+ transference number in liquid electrolytes for better lithium batteries. *Nano Res*. 2023;16(6):8055–8071.
90. Ding LY, Yue XY, Chen YM, Wang ZY, Liu JJ, Shi ZQ, Liang Z. Tandem design of functional separators for Li metal batteries with long-term stability and high-rate capability. *Adv Funct Mater*. 2023;33(43):2304386.
91. Chen DC, Qin ZC, Liang WQ, Wan JL, Liao YH, Li WS. Polyphosphate ester contained flame-retardant separator for interface compatible lithium metal batteries. *J Power Sources*. 2025;641:Article 236908.

92. Zhang C, Li H, Wang S, Cao Y, Yang H, Ai X, Zhong F. A polyethylene microsphere-coated separator with rapid thermal shutdown function for lithium-ion batteries. *J Energy Chem*. 2020;44:33–40.
93. Liu Z, Peng Y, Meng T, Yu L, Wang S, Hu X. Thermal-triggered fire-extinguishing separators by phase change materials for high-safety lithium-ion batteries. *Energy Storage Mater*. 2022;47:445–452.
94. Zheng G, Zeng Z, Shao Z, Shen R, Li H, Jiang J, Wang X, Li W, Liu Y. Coaxial electrospun core-shell lithium-ion battery separator with flame retardant and thermal shutdown functions. *Mater Chem Phys*. 2023;301:Article 127647.
95. Yu Y, Liang Y, You D, Yang W, Zhu Z, Zhang Y, Duan L, Li X, Zhang Y. Construction of a multifunctional separator based on poly(terephthaloyl-melamine) for the thermally safe regulation of lithium-ion batteries. *Molecules*. 2026;31(8):1304.
96. Liu YJ, Tai ZX, Rozen I, Yu ZP, Lu ZY, LaGrow AP, Bondarchuk O, Chen QQ, Goobes G, Li Y, et al. Ion flux regulation through PTFE nanospheres impregnated in glass fiber separators for long-lived lithium and sodium metal batteries. *Adv Energy Mater*. 2023;13(24):2204420.
97. Sun H, Duan F, Zhang T, Cao RQ, Li YP, Cao HB. Dual-functional modification: Improving both thermal stability and wettability of polytetrafluoroethylene composite separators for advanced lithium-ion batteries. *J Energy Storage*. 2026;142:Article 119546.
98. Wang XY, Lin ZY, Fu YX, Chen XY, Chen Y, Yang YF, Li XY, Zeng XY, Wen YF, Yang YC, et al. High-temperature resistant semi-crystalline poly(ether ether ketone) separator. *Energy Storage Mater*. 2025;82:Article 104642.
99. Zhang GH, Xian DX, Hussain S, Zhang B, Lin WJ, Xiang XZ, Wang L. Enhancing lithium metal battery safety and performance: A thermally stable poly(aryl ether benzimidazole) separator with 2D-functionalized boron nitride for 3000 hours lithium plating/stripping. *J Mater Chem A*. 2025;13(6):4486–4495.
100. Zhou KJ, Fang YK, Bao MX, Fan W, Ren JG, He P, Zhang LS, Liu TX. Self-extinguishing polyimide sandwiched separators for high-safety and fast-charging lithium metal batteries. *J Power Sources*. 2024;610:Article 234734.
101. Wang S, Shi H, Xia Y, Liu D, Min C, Zeng M, Liang S, Shao R, Wu X, Xu Z. A 3D-printed framework with a gradient distributed heterojunction and fast Li+ conductivity interfaces for high-rate lithium metal anodes. *J Mater Chem A*. 2022;10(45):24258–24268.
102. Guo JX, Gao C, Liu H, Jiang F, Liu Z, Wang T, Ma Y, Zhong Y, He J, Zhu Z, et al. Inherent thermal-responsive strategies for safe lithium batteries. *J Energy Chem*. 2024;89:519–534.
103. Li P, Liu Z, Peng Y, Yang S, Meng T, Hu Y, Jiang Y, Sun H, Li Q, Hu X. Fast thermal responsive separators toward long-life and safe lithium metal batteries. *Nano Res*. 2024;17(4):2746–2754.
104. Zhang Y, Liu HS, Xie Z, Qu W, Freschi DJ, Liu J. Progress and perspectives of lithium aluminum germanium phosphate-based solid electrolytes for lithium batteries. *Adv Funct Mater*. 2023;33(32):2300973.
105. Cheng H, Yu KZ, Xu DL, Wu GX, Li MH, Wang S, Shen BL, Zhang JY, Huang X, Tian BB. A lithium-poor tantalum oxychloride solid electrolyte for all-solid-state lithium batteries. *Chem Eng J*. 2025;511:Article 162128.
106. Zheng FF, Li CW, Li ZC, Cao X, Luo HB, Liang J, Zhao XD, Kong J. Advanced composite solid electrolytes for lithium batteries: Filler dimensional design and ion path optimization. *Small*. 2023;19(21):2206355.
107. Gomes L, Dai H, Chambers D, Sanctis VR, Yang K, Dong R, Do A, Ji T, Mukerjee S. Solvent dynamics in gel polymer electrolytes for lithium–sulfur batteries. *ACS Nano*. 2025;19(21):19715–19729.
108. Jiang Z, Shi L, Wu M, Jin J, Wen Z. Construction of high-strength flame-retardant Li-SPEEK-modified PEG gel polymer electrolytes for lithium batteries. *ACS Appl Energy Mater*. 2023;6(11):6381–6390.
109. Kim TY, Yun S, Chae JA, Kim HJ, Choi UH. Nanohybrid gel polymer electrolytes based on vinyl-functionalized mesoporous silica nanoparticles for lithium metal batteries. *ACS Appl Energy Mater*. 2023;7(1):48–60.
110. Wei LY, Feng Y, Ge SH, Liu SJ, Ma YY, Yan JH. Three-dimensionally printed ionogel-coated ceramic electrolytes for solid-state lithium batteries. *ACS Nano*. 2025;19(5):5789–5800.
111. Vu TT, Cheon HJ, Shin SY, Jeong G, Wi E, Chang MC. Hybrid electrolytes for solid-state lithium batteries: Challenges, progress, and prospects. *Energy Storage Mater*. 2023;61:Article 102876.
112. Li JW, Li YY, Wang YX, Wang XJ, Wang P, Ci LJ, Liu ZM. Preparation, design and interfacial modification of sulfide solid electrolytes for all-solid-state lithium metal batteries. *Energy Storage Mater*. 2025;74:Article 103962.
113. Wang JC, Zhao LL, Zhang N, Wang PF, Yi TF. Interfacial stability between sulfide solid electrolytes and lithium anodes: Challenges, strategies and perspectives. *Nano Energy*. 2024;123:Article 109361.
114. Yao MX, Shi JT, Luo AH, Zhang ZQ, Zhu GS, Xu HR, Xu JW, Jiang L, Jiang KP. Advances in sulfide solid-state electrolytes for lithium batteries. *Energy Storage Mater*. 2025;75:Article 104018.
115. Barai P, Fuchs T, Trevisanello E, Kim HK, Richter FH, Janek J, Srinivasan V. Reaction current heterogeneity at the interface between a lithium electrode and polymer/ceramic composite electrolytes. *ACS Appl Energy Mater*. 2023;6(4):2160–2177.
116. Du A, Lu HT, Liu SS, Chen SY, Chen ZH, Li WH, Song JW, Yang QH, Yang CP. Breaking the trade-off between ionic conductivity and mechanical strength in solid polymer electrolytes for high-performance solid lithium batteries. *Adv Energy Mater*. 2024;14(31):2400808.
117. Fortuin BA, Meabe L, Peña SR, Zhang Y, Qiao L, Etxabe J, Garcia L, Manzano H, Armand M, Martínez-Ibañez M, et al. Molecular-level insight into charge carrier transport and speciation in solid polymer electrolytes by chemically tuning both polymer and lithium salt. *J Phys Chem C*. 2023;127(4):1955–1964.
118. Liu JJ, Liu X, Chen XW, Zhou JJ, Xue JX, Zhao HJ, Wang C, Liu FQ, Li L. In situ forming asymmetric gel polymer electrolyte enhances the performance of high-voltage lithium metal batteries. *ACS Appl Mater Interfaces*. 2024;16(41):55395–55406.
119. Bertoli L, Gabriele G, Gibertini E, Magagnin L. Unconventional PEO-PPC quasi-solid state blend polymer electrolyte for high efficiency solid-state Li-metal batteries. *J Energy Storage*. 2024;81:Article 110456.

120. Yang ZF, Yang ZH, Liu JX, Ye G, Chen SY, Li RL, Zhang H, Huang TQ, Pang QQ, Liu HT. Self-assembled cluster topology enabled composite solid electrolytes for high-performance lithium metal batteries. *Adv Energy Mater*. 2025;15(41):Article e03760.
121. Guo J, Chen S, Feng F, Wang R, Lai F, Ma Z-F, Hofkens J, Liu T. Fast-ion-conductor multiscale nanoconfinement overcomes ion-transport limitations in all-solid-state sodium batteries. *Adv Mater*. 2026;38(10):Article e18830.
122. Jia ZW, Jia MY, Sun QF, Wang N, Bi ZJ, Guo XX. Configuration design toward sustainably-released polymer electrolytes for enhancing ionic transport and cycle stability of solid lithium batteries. *Energy Storage Mater*. 2024;68:Article 103325.
123. Wang N, Jia MY, Bi ZJ, Guo XX. Composite electrolytes with Li_2CO_3-free garnets achieved by one-step poly(propylene carbonate) treatment for high-rate and long-life solid lithium batteries. *Adv Funct Mater*. 2024;34(37):2401400.
124. Liu TT, Zhong Y, Yan ZW, He BY, Liu T, Ling ZY, Li BC, Liu X, Zhu JL, Jiang LY, et al. Fabrication of scalable covalent organic framework membrane-based electrolytes for solid-state lithium metal batteries. *Angew Chem Int Ed*. 2024;63(50):Article e202411535.
125. Zhang Y, Liu Y, Bao WD, Zhang XY, Yan P, Yao X, Chen MZ, Xie TY, Cao L, Cai XC, et al. Monolithic titanium alkoxide networks for lithium-ion conductive all-solid-state electrolytes. *Nano Lett*. 2023;23(9):4066–4073.
126. Yuan JX, Dong H, Wang B, Qiu M, Liu ZD, Wu XJ, Zhong S, Tong GS, Chen ZY, Zhang JC, et al. Coordination polymer-reinforced composite polymer electrolyte for all-solid-state Li-metal batteries. *Chem Eng J*. 2024;487:Article 150489.
127. Luo P, Su KX, Wu YL, Song X, Huang LZ, Zeng BW, Zhang SC, Liu J, Cui ZM. Solid polymer electrolyte with dual Lewis-acid filler for ultra-stable lithium metal batteries. *Adv Mater*. 2025;37(28):2501142.
128. Lu JQ, Liu QB, Zheng YY, Shi KX, Dang D. Chain-segment ferry engineering from anchoring anion of the composite solid electrolyte enables fast lithium ion transport. *Chem Eng Sci*. 2025;303:Article 120962.
129. Wang JH, Li YP, Tu WB, Zhang HT, Yu XY, Yang YR, Luo HY, Zhao QA, Ru YX, Chen M, et al. Regulating dynamic evolution of interfacial electrolyte configuration via inert cation induced anion anchoring to stabilize lithium-metal anode. *Angew Chem Int Ed*. 2025;64(42):Article e202513839.
130. Liu SJ, Zhao YZ, Zhou L, Chen JJ, Neyts K. Programming ionic landscapes: Ferroelectric liquid crystals, dielectric fields, and process-programmed assembly for the future of solid-state batteries. *Batter Energy*. 2026;5(3):Article e70117.
131. Lou XC, Zhong J, Cheng DP, Han QG, Wang FH, Ji SJ, Sha WX, Wang FQ, Tian J, Zhang WX, et al. Solvent-free quasi-solid polymer electrolyte with a high dielectric constant for stable lithium metal anodes. *Chem Eng J*. 2023;468:Article 143681.
132. Zuo JH, Dang Y, Zhai PB, Li BX, Wang L, Wang MX, Yang ZL, Chen QA, Gu XK, Li ZY, et al. Fast lithium ion transport pathways constructed by two-dimensional boron nitride nanoflakes in quasi-solid-state polymer electrolyte. *Nano Lett*. 2023;23(17):8106–8114.
133. Cui MY, Zhao HY, Qin YY, Zhang SS, Zhao RX, Zhang M, Yu W, Gao GX, Hu XF, Su YQ, et al. Regulation of lithium-ion flux by nanotopology lithiophilic boron-oxygen dipole in solid polymer electrolytes for lithium-metal batteries. *Energy Environ Mater*. 2024;7(4):Article e12659.
134. Yan SS, Wang Z, Liu FX, Zhou HY, Liu K. Aromatic donor-acceptor charge-transfer interactions reinforced supramolecular polymer electrolyte for solid-state lithium batteries. *Adv Funct Mater*. 2023;33(50):2303739.
135. Chen L, Liu X, Zang GJ, Xie JH, Wu BH, Zhang C, Xu Y, Luo YX, Yu DS, Zhang ZS. A new strategy through polymer in situ ionization to construct high-performance electrolyte for solid-state batteries. *J Energy Chem*. 2025;105:814–822.
136. Duan T, Li JM, Li LL, Sun QC, Lu XG, Cheng HW. An oxygen-defective framework with intensified Lewis acidity reinforcing composite electrolyte for all-solid-state lithium metal batteries. *Energy Storage Mater*. 2024;73:Article 103847.
137. Fang Z, Deng QH, Zhou Y, Fu XL, Yi JC, Wu LZ, Dai QY, Yang Y. Pendant length-dependent electrochemical performances for conjugated organic polymers as solid-state polymer electrolytes in lithium metal batteries. *ACS Appl Mater Interfaces*. 2023;15(6):5283–5292.
138. Zou L, Shi K, Liu HL, Wu Y, Xu T, Wang Q, Chen ZX, Yang ZH, Song R, Su JH, et al. Polybenzimidazole-reinforced polyethylene oxide-based polymer-in-salt electrolytes enabling excellent structural stability and superior electrochemical performance for lithium metal batteries. *Chem Eng J*. 2023;465:Article 142794.
139. Zou YL, He YH, Li HY, Deng SY, Tang WH, Deng S. Peo-based electrolyte filled with UV-cured 3D cross-linked polymer network for lithium metal batteries. *J Energy Storage*. 2024;104:Article 114619.
140. Chen X, Kong X. Nanoscale confinement effects on ionic conductivity of solid polymer electrolytes: The interplay between diffusion and dissociation. *Nano Lett*. 2023;23(11):5194–5200.
141. Chen ZH, Jia H, Yan SS, Gohy JF. Polymer-coated silica dual functional fillers to improve the performance of poly(ethylene oxide)-based solid electrolytes. *Nano Energy*. 2023;114:Article 108637.
142. Li XR, Liu S, Shi J, Huang MH, Shi ZC, Wang HL, Yan ZH. High performance porous poly(ethylene oxide)-based composite solid electrolytes. *Chem Eng J*. 2023;468:Article 143795.
143. Shan X, Wei Y, Chen J, Cao P-F. Design principles of ultrathin polymer-based electrolyte for lithium-metal batteries. *J Polym Mater*. 2025;42(3):571–586.
144. Liu L, Mo J, Zhou R, Yang T, Xu R, Tu J, Zhao Q, Zhang M, Zhang D, Wang B, et al. Ultrathin solid composite electrolytes for long-life lithium metal batteries. *J Energy Storage*. 2025;114:Article 115777.
145. Ma Y, Wan J, Yang Y, Ye Y, Xiao X, Boyle DT, Burke W, Huang Z, Chen H, Cui Y, et al. Scalable, ultrathin, and high-temperature-resistant solid polymer electrolytes for energy-dense lithium metal batteries. *Adv Energy Mater*. 2022;12(15):2103720.
146. Liu Y, Wang P, Yang Z, Wang L, Li Z, Liu C, Liu B, Sun Z, Pei H, Lv Z, et al. Lignin derived ultrathin all-solid polymer electrolytes with 3D single-ion nanofiber ionic bridge framework for high performance lithium batteries. *Adv Mater*. 2024;36(27):2400970.
147. Wang D, Zhang Y, Tang J, Huang J, Chen X, Tang M, Wang Z. Ultrathin polymer composite electrolyte with dual-scale reinforcement: Integrating ptfe framework and in situ silica. *Polym Eng Sci*. 2026;66(4):2901–2909.

148. Liang Q, Chen L, Tang J, Liu X, Liu J, Tang M, Wang Z. Large-scale preparation of ultrathin composite polymer electrolytes with excellent mechanical properties and high thermal stability for solid-state lithium-metal batteries. *Energy Storage Mater*. 2023;55:847–856.
149. Feng J, Wang J, Gu Q, Thitisomboon W, Yao D, Deng Y, Gao P. Room-temperature all-solid-state lithium metal batteries based on ultrathin polymeric electrolytes. *J Mater Chem A*. 2022;10(26):13969–13977.
150. Shao LZ, Tang JY, Fang SY, Zhang YF, Peng D, Huang JM, Tang M, Wang ZB. Regulation of the ionic transport and electrochemical stability in poly(ethylene oxide) solid electrolyte via terminal polyfluorinated modification. *ACS Appl Mater Interfaces*. 2025;17(46):63353–63362.
151. Huang B, Chen SJ, Zeng PJ, Song LX, Wei ZQ, Zhu HL, Guo YH. Polyethylene oxide/polytetrafluoroethylene-based dual lithium salt composite solid-state electrolyte membrane for solid-state lithium metal batteries. *J Energy Storage*. 2025;135:Article 118373.
152. Xie KC, Shi LX. Ultrathin PEO based electrolyte for high voltage lithium metal batteries enabled by polymer host-plasticizer interactions. *J Energy Storage*. 2023;68: Article 107640.
153. Monroe C, Newman J. The impact of elastic deformation on deposition kinetics at lithium/polymer interfaces. *J Electrochem Soc*. 2005;152(2):A396–A404.
154. Hu XY, Zhang BQ. Reinforced flexible solid-state electrolyte membrane by polyurethane polymer of intrinsic microporosity for high-energy-density lithium metal battery. *J Membr Sci*. 2024;701:Article 122710.
155. Yuan SD, Luo Y, Xia K, Zheng AQ, Jiang GD, Fan MX, Xiong J, Yuan CC, Li ZG, Wang XB. Developing flexible and safety-reinforced 3D polymer electrolytes based on polyethylene oxide for solid-state lithium metal batteries. *J Energy Storage*. 2024;78:Article 109853.
156. Yang X, Fang L, Li J, Liu C, Zhong LF, Yang F, Wang XT, Zhang ZS, Yu DS. Multipolar conjugated polymer framework derived ionic sieves via electronic modulation for long-life all-solid-state Li batteries. *Angew Chem Int Ed*. 2024;63(23):Article e202401957.
157. Zhang Y, Lou X, Dan J, Franke C, Tang L, Li J, Gao Z, Zhou L, Chen B, Li T, et al. Coupling alloyed lean lithium anodes with pim-1-blended PEO electrolytes synergistically promotes reversible Li stripping/deposition reactions for all-solid-state lithium-metal batteries. *J Energy Storage*. 2024;94: Article 112399.
158. Liu P, Zhong L, Wang SJ, Huang S, Han DM, Huang ZH, Xiao M, Meng YZ. Ultra-long-life and ultrathin quasi-solid electrolytes fabricated by solvent-free technology for safe lithium metal batteries. *Energy Storage Mater*. 2023;58:132–141.
159. Liu YY, Han LF, Liao C, Yu H, Kan YC, Hu Y. Ultra-thin, non-combustible PEO polymer solid electrolyte for high safety polymer lithium metal batteries. *Chem Eng J*. 2023;468: Article 143222.
160. Cao YK, Liu YY, Cheng LY, Han LF, Kan YC, Hu Y. Non-flammable, ultra-thin, high-performance PEO-based polymer electrolyte for lithium metal batteries. *Chem Eng J*. 2025;524:Article 169042.
161. Sarmad B, Gao L, Kang WM. Preparation and application of polyacrylonitrile electrospun nanofiber-based all-solid-state composite electrolyte for lithium metal battery. *Polymer*. 2023;285:Article 126275.
162. Song JC, Xu YX, Zhou YC, Wang PF, Feng HL, Yang J, Tan QQ, Zhuge FC. Cellulose-assisted vertically heterostructured PEO-based solid electrolytes mitigating Li-succinonitrile corrosion for lithium metal batteries. *ACS Appl Mater Interfaces*. 2023;15(17):20897–20908.
163. Zhang H, Fu Y, Wang S. Numerical simulation of key factors affecting dendrite growth in solid-state electrolyte batteries under multi-physical coupling fields. *J Energy Storage*. 2026;141:Article 119364.
164. Zheng JA, Liu SJ, Huang H, Zhou HX, Li HY, Li LX, Jiang GS, Zhang H, Geng X, An BG, et al. Heterocyclic polymer supported cathode/Li interface layers to lower the operational temperature of PEO-based Li-batteries. *Nano Energy*. 2023;118:Article 108975.
165. Liang WZ, Zhou XY, Zhang B, Zhao ZS, Song X, Chen K, Wang L, Ma ZS, Liu J. The versatile establishment of charge storage in polymer solid electrolyte with enhanced charge transfer for LiF-rich SEI generation in lithium metal batteries. *Angew Chem Int Ed*. 2024;63(18): Article e202320149.
166. Zhou S, Zhu YT, Hu HR, Li CH, Jiang J, Huang JY, Zhang B. Tuning the LiF content in the SEI by engineering the molecular structures of porous organic polymers for solid-state lithium metal batteries. *J Mater Chem A*. 2023;11(11):5636–5644.
167. Yang Q, Liao MM, Ren PF, Li DQ, Deng NP, Kang WM, Cai GM. Dual functional composite solid electrolyte constructed by double-layer sulfonated polyethersulfone (spes)/poly(vinylidene fluoride-co-hexafluoropropylene) (PVDF-HFP) nanofiber membrane in high-performance all-solid-state lithium metal batteries. *Chem Eng J*. 2024;495:Article 153448.
168. Gao LJ, Jiang WB, Zhang XR, Sun YX, Chen K, Li WL, Xie HM, Liu J. A self-healing poly(ionic liquid) block copolymer electrolyte enabled by synergetic dual ion-dipole interactions. *Chem Eng J*. 2024;479:Article 147822.
169. Chen YT, Paste R, Lin HC, Chu CW. Self-curing solid-state electrolytes based on transamination bond exchange for reliable lithium batteries. *J Mater Chem A*. 2023;11(43):23536–23546.
170. Wu K, Ju Z, Zhang B, Marschilok AC, Takeuchi ES, Takeuchi KJ, Yu G. In situ alloying enabled by active liquid metal filler for self-healing composite polymer electrolytes. *Angew Chem Int Ed*. 2024;63(47):Article e202410463.
171. Huang ZX, Zhang T, Zhang ZP, Rong MZ, Zhang MQ. Highly ionic conductive, self-healing, $Li_{10}GeP_2S_{12}$-filled composite solid electrolytes based on reversibly interlocked macromolecule networks for lithium metal batteries with improved cycling stability. *ACS Appl Mater Interfaces*. 2024;16(32):42736–42747.
172. Lu Y-H, Liu Y-L. Self-healing and externally recoverable solid polymer electrolytes for lithium metal batteries with enhanced cycling stability. *ACS Appl Energy Mater*. 2026;9:7803–7812.
173. Ma Y, Zhang R, Wang L, Wu J, Chen B, Yu Y, Li L, He F, Shi C, Zhao N, et al. Self-healing polymer-based electrolyte induced by amorphous three-dimensional carbon for high-performance solid-state Li metal batteries. *Energy Storage Mater*. 2023;61:Article 102893.
174. Liu LQ, Zhu LF, Wang YL, Guan XW, Zhang ZF, Li H, Wang F, Zhang H, Zhang Z, Yang ZY, et al. Starfish-inspired solid-state Li-ion conductive membrane with balanced

rigidity and flexibility for ultrastable lithium metal batteries. *Angew Chem Int Ed*. 2025;64(7):Article e202420001.
175. Li T, Panda PK, Hsieh CT, Gandomi YA, Yang PC. Lithium iron phosphate cathode supported solid lithium batteries with dual composite solid electrolytes enabling high energy density and stable cyclability. *J Energy Storage*. 2024;81: Article 110444.
176. Wang S, Sun QF, Zhang Q, Li C, Xu CR, Ma Y, Shi XX, Zhang HZ, Song DW, Zhang LQ. Li-ion transfer mechanism of ambient-temperature solid polymer electrolyte toward lithium metal battery. *Adv Energy Mater*. 2023;13(16):2204036.
177. Yang JR, Liu JZ, Cai WR, Zhao ZY, Wang S, He L, Lv SS, Zhu ZW, Ji ZF, Wen GJ, et al. A self-adaptive inorganic in-situ separator by particle crosslinking for nonflammable lithium-ion batteries. *J Energy Chem*. 2025;100:469–480.
178. Wang XW, Wang MH, Chen HL, Zhang YY, Niu B, Tian LY, Long DH. Dynamically reversible cross-linked polymer electrolytes with highly ionic conductivity for dendrite-free lithium metal batteries. *Chem Eng J*. 2024;496:Article 153830.